Fraunhofer Institut Techno- und Wirtschaftsmathematik

ITWM

R. Ewing, O. Iliev, R. Lazarov, A. Naumovich

On convergence of certain finite difference discretizations for 1D poroelasticity interface problems

Berichte des Fraunhofer ITWM, Nr. 69 (2004)

ISSN 1434-9973

Bericht 69 (2004)

Die Veröffentlichungen in der Berichtsreihe des Fraunhofer ITWM können bezogen werden über:

Fraunhofer-Institut für Techno- und
Wirtschaftsmathematik ITWM
Gottlieb-Daimler-Straße, Geb. 49

67663 Kaiserslautern
Germany

Telefon: +49 (0) 6 31/2 05-32 42
Telefax: +49 (0) 6 31/2 05-41 39
E-Mail: info@itwm.fraunhofer.de
Internet: www.itwm.fraunhofer.de

Vorwort

Das Tätigkeitsfeld des Fraunhofer Instituts für Techno- und Wirtschaftsmathematik ITWM umfasst anwendungsnahe Grundlagenforschung, angewandte Forschung sowie Beratung und kundenspezifische Lösungen auf allen Gebieten, die für Techno- und Wirtschaftsmathematik bedeutsam sind.

In der Reihe »Berichte des Fraunhofer ITWM« soll die Arbeit des Instituts kontinuierlich einer interessierten Öffentlichkeit in Industrie, Wirtschaft und Wissenschaft vorgestellt werden. Durch die enge Verzahnung mit dem Fachbereich Mathematik der Universität Kaiserslautern sowie durch zahlreiche Kooperationen mit internationalen Institutionen und Hochschulen in den Bereichen Ausbildung und Forschung ist ein großes Potenzial für Forschungsberichte vorhanden. In die Berichtreihe sollen sowohl hervorragende Diplom- und Projektarbeiten und Dissertationen als auch Forschungsberichte der Institutsmitarbeiter und Institutsgäste zu aktuellen Fragen der Techno- und Wirtschaftsmathematik aufgenommen werden.

Darüberhinaus bietet die Reihe ein Forum für die Berichterstattung über die zahlreichen Kooperationsprojekte des Instituts mit Partnern aus Industrie und Wirtschaft.

Berichterstattung heißt hier Dokumentation darüber, wie aktuelle Ergebnisse aus mathematischer Forschungs- und Entwicklungsarbeit in industrielle Anwendungen und Softwareprodukte transferiert werden, und wie umgekehrt Probleme der Praxis neue interessante mathematische Fragestellungen generieren.

Prof. Dr. Dieter Prätzel-Wolters
Institutsleiter

Kaiserslautern, im Juni 2001

On convergence of certain finite difference discretizations for 1-D poroelasticity interface problems

R.Ewing,
Inst. for Scientific Computing, Texas A&M University,
College Station, TX 77843, USA
ewing@tamu.edu

O.Iliev
Fraunhofer Institut fuer Techno- und Wirtschaftsmathematik,
Gottlieb-Daimler Str. Geb.49, 67663 Kaiserslautern, Germany
iliev@itwm.fhg.de

R.Lazarov,
Dept. of Mathematics, Texas A&M University,
College Station, TX 77843, USA,
lazarov@math.tamu.edu

A.Naumovich,
Fraunhofer Institut fuer Techno- und Wirtschaftsmathematik,
Gottlieb-Daimler Str. Geb.49, 67663 Kaiserslautern, Germany
naumovic@itwm.fhg.de

Keywords: poroelasticity, multilayered material, finite volume discretizations, MAC type grid, error estimates

Abstract

Finite difference discretizations of 1-D poroelasticity equations with discontinuous coefficients are analyzed. A recently suggested FD discretization of poroelasticity equations with constant coefficients on staggered grid, [5], is used as a basis. A careful treatment of the interfaces leads to harmonic averaging of the discontinuous coefficients. Here, convergence for the pressure and for the displacement is proven in certain norms for the scheme with harmonic averaging (HA). Order of convergence 1.5 is proven for arbitrary located interface, and second order convergence is proven for the case when the interface coincides with a grid node. Furthermore, following the ideas from [3], modified HA discretization are suggested for particular cases. The velocity and the stress are approximated with second order on the interface in this case. It is shown that for wide class of problems, the modified discretization provides better accuracy. Second order convergence for modified scheme is proven for the case when the interface coincides with a displacement grid node. Numerical experiments are presented in order to illustrate our considerations.

1 Introduction

Recently, there is a growing interest in numerical approaches for solving poroelasticity equations. The derived by Biot model [1] (see also [2, 7] and references therein) describes well a class of flows in deformable porous media, which is of interest for geosciences, bioscience, engineering, etc. Analysis of the well-posedness (uniqueness and existence of the solution) of this problem can be found, for example, in [11]. The classical Biot model treats consolidation of linearly elastic porous solid domain $\Omega \subset R^d$ with boundary Γ, which either is saturated by a slightly compressible fluid, or is almost saturated with incompressible fluid. The fluid pressure $p(x,t)$ and the displacement of the media $\mathbf{u} = (u_1, \ldots, u_d)$ satisfy the following system

$$-\nabla \cdot \sigma + \alpha \nabla p = \mathbf{f}(x,t),$$

$$\frac{\partial}{\partial t}(c_0 p + \alpha \nabla \cdot \mathbf{u}) - \nabla \cdot (k \nabla p) = h(x,t),$$

consisting of the equilibrium equation for the momentum and the diffusion equation for the Darcy flow. The constant $c_0 > 0$ combines compressibility of the fluid and porosity, while the coefficient $k > 0$ involves the permeability and the viscosity of the fluid as a measure of the Darcy flow corresponding to a pressure gradient. The term $\alpha \nabla p$ in the first equation results from the additional stress of the fluid pressure within the structure and $\alpha \nabla \cdot \mathbf{u}$ in the second equation represents the additional fluid content due to local volume change. Here $\sigma = \sigma(\mathbf{u})$ is the stress tensor (a symmetric $d \times d$ tensor with components $\sigma_{ij},\ i,j = 1, \ldots, d$) which is related to the small strain tensor $\varepsilon = \varepsilon(\mathbf{u})$ with components $\varepsilon_{ij} = \frac{1}{2}(\frac{\partial u_i}{\partial x_j} + \frac{\partial u_j}{\partial x_i}),\ i,j = 1, \ldots, d$ via the linear stress-strain relations (Hook's law) $\sigma_{ij} = 2\mu\varepsilon_{ij} + \lambda \nabla \cdot \mathbf{u} \delta_{ij},\ i,j = 1, \ldots, d$. Here $\mu = \mu(x) > 0$ (shear moduli) and $\lambda = \lambda(x) > 0$ (dilation) are the Lamé coefficients of the elastic media (in general piece-wise smooth functions, e.g. piece-wise constants). Above $\nabla \cdot \sigma$ denotes a vector with $i-$th component $\sum_{j=1}^{d} \frac{\partial \sigma_{ij}}{\partial x_j}$. This system is supplied with relevant boundary conditions that have clear physical meaning. For example, the pressure $p = g$ could be prescribed on part of the boundary Γ_D and "no-flow" condition $k \nabla p \cdot \mathbf{n} = 0$ on the rest of the boundary Γ_N. Here $\mathbf{n}$ is the unit normal vector to Γ, pointing outside the domain Ω. For the displacement we may have $\mathbf{u} = 0$ on Γ_0 and $\sigma \cdot \mathbf{n} = \mathbf{g}$ on Γ_t that corresponds to the case when the elastic body is clamped on Γ_0 and have prescribed traction force on Γ_t.

This system is remarkable in many respects. First, it is a good approximation of a physical process for which the deformations vary sufficiently slowly that the inertia effects are negligible. Second, it is a reasonable simplification of more general systems that model barotropic fluids, $\rho = \rho(p)$, and/or partially saturated porous media which involves additional variable, the saturation S and uses one more equation. This and other models are important tools for computer simulations of flow in porous media and lead to many interesting applications.

Analytical solution of Biot system is available only in very special cases, therefore numerical methods are usually used for solving the respective initial-boundary value problem. FEM is preferred from the most of researchers and practitioners who deal with poroelasticity equations. However, FEM solution (as well as FDM solution on collocated grids) is a subject of non-physical oscillations at the early stages of calculations (i.e., close to the initial state). To avoid this, FD discretization on staggered grid is suggested and theoretically analyzed in [5, 6]. According to the grid and operator notations introduced in the third section below, finite difference schemes approximating the above IVP can be written in the operator form as follows

$$\begin{aligned}
&Au^{j+1} + Gp^{j+1} = 0,\ j = 0, 1, \ldots, M-1,\\
&\left(Qp^j + Du^j\right)_t + Bp^j_\sigma = f^j_\sigma,\ \ j = 0, 1, \ldots, M-1,\\
&p_0^{j+1} = 0,\ u_N^{j+1} = 0,\ \ j = 0, 1, \ldots, M-1,\\
&Qp^0 + Du^0 = \tfrac{1}{\nu},\ \ j = 0.
\end{aligned}$$

The operators A, B, G, D, Q are defined in different way for the case of continuous coefficients and for the case of discontinuous coefficients (the last case further distinguishes between scheme based on harmonic averaging, and modified HA scheme). However, in all the cases A and B are self-adjoint and positive definite operators, while G and D are adjoint to each other with respect to proper inner product. In the case of continuous coefficients in Biot system (single layered porous media), second order convergence in operator norms is proven in [5]. In this paper we present theoretical analysis of certain FD schemes in the case of discontinuous coefficients. FD schemes for poroelasticity equations with discontinuous coefficients are often used in practice, but up to our knowledge, there is no systematic analysis of their convergence. A scheme for multilayered porous domain is discussed in [8], and a number of numerical experiments are presented there in order to demonstrate its accuracy. The finite volume method (method of the balance, [9]) is used there, what results in harmonic averaging for the discontinuous coefficients. For this scheme we prove here convergence with $O(h^{\frac{3}{2}})$ in operator norms in the case of arbitrary location of the interface, and convergence with $O(h^2)$ when the interface coincides with grid nodes associated with displacements. Furthermore, we present here a modified harmonic averaging scheme for the system of poroelasticity equations. The last is motivated by a similar approach, applied earlier (see [3]) to a scalar equation with discontinuous coefficients. For the modified HA scheme, we prove convergence with $O(h^2)$ in the case when the interface coincides with a displacement grid node. The proof here is easier, compared to the one for the HA scheme, due to the better approximation for fluxes.

The remainder of the text is organized as follows. Biot model, describing poroelasticity of a multilayered porous media, is presented in the next section. Third section is devoted to presentation and analysis of the scheme using harmonic averaging. Consecutively, staggered grid discretization, operational form of the discretized system, and convergence proofs, are presented there. The fourth section contains derivation and theoretical analysis of modified finite volume discretization, which exploits the equations on the interface in order to increase the order of approximation near the interface. Finally, some conclusions are drawn.

2 Continuous problem formulation

In this paper we deal with an interface problem for one-dimensional model of poroelasticity. It is a system of partial differential equations for fluid pressure, $p = p(x,t)$, and for displacement of the solid skeleton, $u = u(x,t)$, supplemented with necessary boundary, initial and interface conditions

$$-\frac{\partial}{\partial x}\left((\lambda + 2\mu)\frac{\partial u}{\partial x}\right) + \frac{\partial p}{\partial x} = 0,\ x \in (0,l),\ t \in (0,T], \tag{1}$$

$$\frac{\partial}{\partial t}\left(\phi\beta p + \frac{\partial u}{\partial x}\right) - \frac{\partial}{\partial x}\left(\frac{k}{\eta}\frac{\partial p}{\partial x}\right) = f(x,t),\ x \in (0,l),\ t \in (0,T], \tag{2}$$

$$p = 0,\ (\lambda + 2\mu)\frac{\partial u}{\partial x} = -u_0,\ \text{if } x = 0, \tag{3}$$

$$u = 0,\ \frac{\partial p}{\partial x} = 0,\ \text{if } x = l, \tag{4}$$

$$\phi\beta p + \frac{\partial u}{\partial x} = 0,\ \text{for } t = 0 \tag{5}$$

$$[u] = 0,\ \left[(\lambda + 2\mu)\frac{\partial u}{\partial x}\right] = 0,\ [p] = 0,\ \left[\frac{k}{\eta}\frac{\partial p}{\partial x}\right] = 0\ \text{ for } x = \zeta,\ t \in [0, T]. \tag{6}$$

Here λ and μ are Lame coefficients of the solid skeleton, ϕ is porosity, β is compressibility of the fluid, k is permeability, η is viscosity of the fluid, $f(x,t)$ is a source term, and ζ, $0 \le \zeta \le l$, is an interface position.

Coefficients of the governing equations may be discontinuous across the interface, i.e.

$$\lambda = \begin{cases} \lambda_1, & x < \zeta, \\ \lambda_2, & x > \zeta, \end{cases} \quad \mu = \begin{cases} \mu_1, & x < \zeta, \\ \mu_2, & x > \zeta, \end{cases} \quad k = \begin{cases} k_1, & x < \zeta, \\ k_2, & x > \zeta, \end{cases} \quad \phi = \begin{cases} \phi_1, & x < \zeta, \\ \phi_2, & x > \zeta. \end{cases}$$

We give the system (1)-(6) another form by introducing the following dimensionless independent and dependent variables:

$$\tilde{x} := \frac{x}{l}, \quad \tilde{t} := \frac{(\lambda_1 + 2\mu_1)k_1 t}{\eta l^2}, \quad \tilde{p} := \frac{p}{u_0}, \quad \tilde{u} := \frac{(\lambda_1 + 2\mu_1)u}{u_0 l},\ \nu := \frac{\lambda + 2\mu}{\lambda_1 + 2\mu_1}, \quad \tilde{k} := \frac{k}{k_1}.$$

Omitting ˜ from dimensionless variables, using the notations $a = \phi\beta(\lambda_1 + 2\mu_1)$, $\tilde{f}(x,t) = \frac{l^2\eta}{u_0 k_1} f(x,t)$, and making the substitution

$$u = \begin{cases} u + \dfrac{x}{\nu_1} + \dfrac{\zeta}{\nu_2} - \dfrac{1}{\nu_2} - \dfrac{\zeta}{\nu_1}, & x < \zeta, \\ u + \dfrac{x}{\nu_2} - \dfrac{1}{\nu_2}, & x > \zeta \end{cases}$$

we obtain the following problem with homogeneous boundary conditions:

$$\begin{aligned} -\frac{\partial}{\partial x}\left(\nu\frac{\partial u}{\partial x}\right) + \frac{\partial p}{\partial x} &= 0,\ x \in (0,1),\ t \in (0,T], \\ \frac{\partial}{\partial t}\left(ap + \frac{\partial u}{\partial x}\right) - \frac{\partial}{\partial x}\left(k\frac{\partial p}{\partial x}\right) &= f(x,t),\ x \in (0,1),\ t \in (0,T], \\ \nu\frac{\partial u}{\partial x} = 0,\ p = 0, &\quad \text{if } x = 0,\ t \in [0,T], \\ u = 0,\ \frac{\partial p}{\partial x} = 0, &\quad \text{if } x = 1,\ t \in [0,T], \\ ap + \frac{\partial u}{\partial x} = \frac{1}{\nu}, &\quad \text{if } t = 0,\ x \in (0,1), \\ [u] = 0,\ \left[\nu\frac{\partial u}{\partial x}\right] = 0,\ [p] = 0,\ \left[k\frac{\partial p}{\partial x}\right] = 0, &\quad \text{for } x = \zeta,\ t \in [0,T], \end{aligned} \tag{7}$$

where

$$\nu = \begin{cases} 1, & x < \zeta, \\ \nu_2, & x > \zeta, \end{cases} \quad a = \begin{cases} a_1, & x < \zeta, \\ a_2, & x > \zeta, \end{cases} \quad k = \begin{cases} 1, & x < \zeta, \\ k_2, & x > \zeta. \end{cases}$$

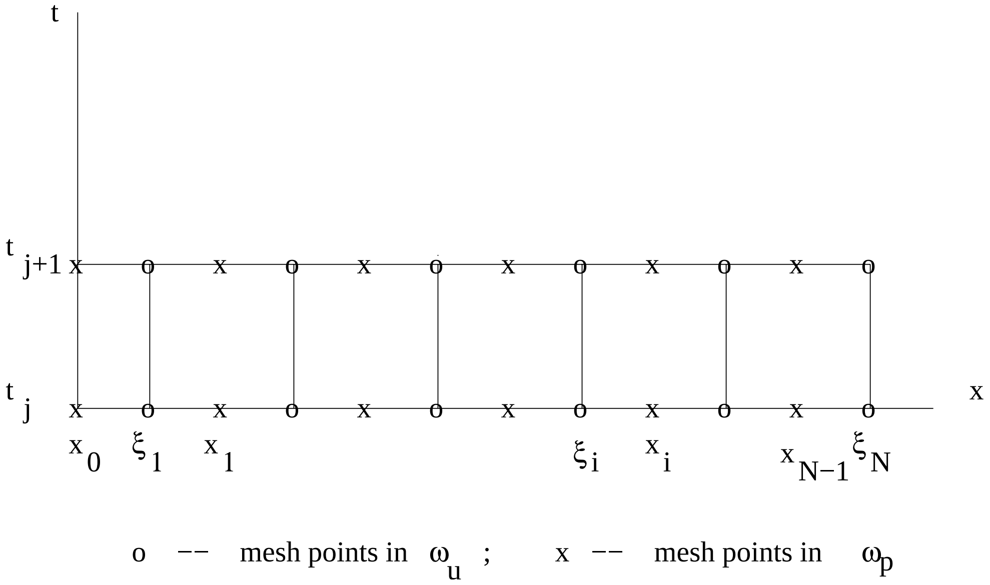

Figure 1: Meshes

3 Finite volume discretization based on harmonic averaging.

3.1 Grids and notations

We split the interval $(0,1)$ into $N > 1$ equal subintervals of size $h = 2/(2N-1)$. We use different spacial grids (so-called staggered grids), $\overline{\omega}_p$ to discretize with respect to pressure, and $\overline{\omega}_u$ to discretize with respect to displacement, and a grid in time t with a step-size τ:

$$\begin{aligned} &\overline{\omega}_p = \{x_i : \ x_i = ih, \ i = 0, \dots, N-1\}\,, \ \omega_p = \{x_i \in \overline{\omega}_p, \ i = 1, \dots, N-1\}\,, \\ &\overline{\omega}_u = \{\xi_i : \ \xi_i = x_i - 0.5h, \ i = 1, \dots, N\}\,, \ \omega_u = \{\xi_i \in \overline{\omega}_u, \ i = 1, \dots, N-1\}\,, \\ &\omega_T = \{t_j : \ t_j = j\tau, \ j = 1, 2, \dots, M\}\,. \end{aligned} \tag{8}$$

One may consider these meshes as designed to represent the values of the pressure p at the grid points $x_i \in \overline{\omega}_p$ and the values of the displacement u at the midpoints $\xi_i \in \overline{\omega}_u$ of the subintervals (x_{i-1}, x_i). Now the position of the interface ζ could be represented in the form

$$\zeta = \xi_n + \theta h, \tag{9}$$

where $0 < n < N$ is an integer and $0 \le \theta < 1$.

Now we shall introduce the following shorthand notations for discrete functions defined on $\overline{\omega}_p \times \omega_T$ and $\overline{\omega}_u \times \omega_T$, respectively:

$$u := u^j := u_i^j := u(\xi_i, t_j), \ p := p^j := p_i^j := p(x_i, t_j), \ v^\sigma := \sigma v^{j+1} + (1-\sigma) v^j, \ \hat{v} := v^{j+1}.$$

Further, we shall use the standard notation for the first order backward and forward finite differences on a uniform mesh (see, e.g.. [9]):

$$p_x := p_{x,i} = (p(x_{i+1}) - p(x_i))/h, \quad p_{\bar{x}} := p_{\bar{x},i} = (p(x_i) - p(x_{i-1}))/h.$$

Inspecting these expressions we see that these differences represent central differences with respect to the points in ω_u and therefore we can easily accept that these represent quantities defined on the mesh ω_u. In a similar way we define

$$u_x := u_{x,i} = (u(\xi_{i+1}) - u(\xi_i))/h, \quad u_{\bar{x}} := u_{\bar{x},i} = (u(\xi_i) - u(\xi_{i-1}))/h,$$

which represent central differences with respect to the points in ω_p and therefore they represent quantities defined on the mesh ω_p . Finally, we define the finite differences in time direction

$$u_t := u_t(\xi_i, t_j) = (u_i^{j+1} - u_i^j)/\tau, \quad \xi_i \in \omega_u, \quad p_t := p_t(x_i, t_j) = (p_i^{j+1} - p_i^j)/\tau, \quad x_i \in \omega_p.$$

Following the basic principles of the finite volume method, we derive finite-difference approximation of problem (7). The approximate solution $u = u_i^j = u(\xi_i, t_j)$, $p = p_i^j = (x_i, t_j)$ satisfies the following difference equations:

$$\begin{aligned}
&-\tfrac{\nu}{h}\hat{u}_x + \hat{p}_x = 0\ , \quad \xi = \xi_1, && t \in \omega_T \quad (i.e.\ i = 1),\\
&-(\nu \hat{u}_{\bar{x}})_x + \hat{p}_x = 0\ , \quad \xi = \xi_i \in \omega_u \backslash \{\xi_1\}, && t \in \omega_T \quad (i.e.\ i = 2, \dots, N-1),\\
&(ap + u_x)_t - (k p_{\bar{x}}^\sigma)_x = f^\sigma, \quad x = x_i \in \omega_p \backslash \{\xi_{N-1}\}, && t \in \omega_T \quad (i.e.\ i = 1, \dots, N-2),\\
&(ap + u_x)_t - \tfrac{k}{h} p_{\bar{x}}^\sigma = f^\sigma, \quad x = x_{N-1}, && t \in \omega_T \quad (i.e.\ i = N-1),\\
&p_0 = 0, \quad u_N = 0, && t \in \omega_T,\\
&ap + u_x = \tfrac{1}{\nu}, \quad x = x_i \in \bar{\omega}_p, && t = 0, \quad (i.e.\ i = 1, \dots, N-1),
\end{aligned} \tag{10}$$

where

$$\nu_i = \left(\frac{1}{h} \int_{\xi_i}^{\xi_{i+1}} \frac{dx}{\nu(x)} \right)^{-1}, \quad k_i = \left(\frac{1}{h} \int_{x_{i-1}}^{x_i} \frac{dx}{k(x)} \right)^{-1}, \tag{11}$$

$$a_i = \frac{1}{h} \int_{\xi_i}^{\xi_{i+1}} a(x)dx, \quad \phi_i = \frac{1}{h} \int_{\xi_i}^{\xi_{i+1}} f(x,t)dx. \tag{12}$$

3.2 Grid operators and operator form of the difference scheme

We introduce Hilbert space $H_{\overline{\omega}_p}$ of discrete functions $p = (p_0, p_1, ..., p_{N-1})$ defined on the grid $\overline{\omega}_p$ and Hilbert space $H_{\overline{\omega}_u}$ of functions $u = (u_1, u_2, ..., u_N)$ defined on the grid $\overline{\omega}_u$. Respective inner products in these spaces are

$$[p, q) = (p, q)_{\overline{\omega}_p} = \sum_{i=0}^{N-1} h p_i q_i, \ (u, v] = (u, v)_{\overline{\omega}_u} = \sum_{i=1}^{N} h u_i v_i,$$

We also introduce Hilbert spaces H_{ω_p} and H_{ω_u} of grid functions $p = (p_1, p_2, ..., p_{N-1})$ and $u = (u_1, u_2, ..., u_{N-1})$ defined on the grids ω_p and ω_u respectively with following inner products

$$(p, q) = (p, q)_{\omega_p} = \sum_{i=1}^{N-1} hp_i q_i, \ (u, v) = (u, v)_{\omega_u} = \sum_{i=1}^{N-1} hu_i v_i.$$

Now we define discrete operators $A : H_{\omega_u} \to H_{\omega_u}$ and $B : H_{\omega_p} \to H_{\omega_p}$

$$(Au)(\xi) = \begin{cases} -\frac{1}{h}\nu_1 u_{\bar{x},2}, & \text{for } \ \xi = \xi_1 \ \ (i.e. \ \ i = 1), \\ -(\nu u_{\bar{x}})_x, \ \text{for} \ \ \xi \in \omega_u \setminus \{\xi_1, \xi_{N-1}\} \ \ (i.e. \ \ i = 2, \dots, N-2) \\ -\frac{\nu_2}{h}(\frac{u_{N-1}}{h} - u_{\bar{x},N-1}), & \text{for } \xi = \xi_{N-1} \ (i.e. \ \ i = N-1). \end{cases}$$

$$(Bp)(x) = \begin{cases} -\frac{k_1}{h}(p_{\bar{x},2} - \frac{p_1}{h}), & \text{for } x = x_1, \ (i.e. \ \ i = 1), \\ -(kp_{\bar{x}})_x \ , \ \ \text{for} \ \ x \in \omega_p \setminus \{x_1, x_{N-1}\} \ \ (i.e. \ \ i = 2, \dots, N-2) \\ \frac{1}{h}(kp_{\bar{x}}) \ , & \text{for} \ \ x = x_{N-1}, \ \ (i.e. \ \ i = N-1). \end{cases}$$

Operators A and B are self-adjoint and positive definite in the inner products of the spaces H_{ω_u} and H_{ω_p} respectively and therefore they define the operator norms:

$$\| u \|_A = (u, u)_A^{1/2}, \quad \| p \|_B = (p, p)_B^{1/2},$$

where inner products are defined as $(u, v)_A = (Au, v)_{\omega_u}$ and $(p, q)_B = (Bp, q)_{\omega_p}$.

Next, we define following operators: the discrete divergence $D : H_{\omega_u} \to H_{\omega_p}$, and the discrete gradient $G : H_{\omega_p} \to H_{\omega_u}$:

$$(Du)_i = (Du)(x_i) = \begin{cases} u_{x,i}, & \text{for } \ i = 1, \dots, N-2, \\ -\frac{u_{N-1}}{h}, & \text{for } i = N-1. \end{cases} \tag{13}$$

$$(Gp)_i = (Gp)(\xi_i) = \begin{cases} \frac{p_1}{h}, & \text{for } i = 1, \\ p_{\bar{x},i}, & \text{for } i = 2, \dots, N-1. \end{cases} \tag{14}$$

One can easily show that for any discrete functions $u \in H_{\omega_u}$, $p \in H_{\omega_p}$, operators G and D satisfy adjoint condition $(Gp, u)_{\omega_u} = -(p, Du)_{\omega_p}$. We also introduce multiplications by a scalar grid functions: $Q : H_{\omega_p} \to H_{\omega_p}$, $N : H_{\omega_p} \to H_{\omega_p}$ and $K : H_{\omega_u} \to H_{\omega_u}$

$$(Qp)_i = (Qp)(x_i) = a_i p_i, \quad x \in \omega_p,$$

$$(Nq)_i = (Nq)(x_i) = \nu_i q_i, \quad x \in \omega_p,$$

$$(Kw)_i = (Kw)(\xi_i) = k_i w_i, \quad \xi \in \omega_u.$$

Note, following representations are valid for operators A and B :

$$A = -GND,$$

and

$$B = -DKG.$$

For the further analysis we will need some properties of the operators and operator norms introduced above. These properties we formulate with the following lemmas:

Lemma 1.
For any grid function g, defined on the grid ω_u, following estimate is valid:

$$\|Dg\| \leq c_\nu \|g\|_A, \tag{15}$$

where $c_\nu = (\min\{\nu_1, \nu_2\})^{-1/2}$.

Proof. According to the definition

$$\|g\|_A^2 = (Ag, g) = -(GNDg, g) = (NDg, Dg) \geq \min\{\nu_1, \nu_2\}(Dg, Dg) = \min\{\nu_1, \nu_2\}\|Dg\|^2,$$

from where follows an estimate (15). □

Lemma 2.
For any grid function q, defined on the grid ω_p, following estimate is valid:

$$\|Gq\| \leq c_k \|q\|_B, \tag{16}$$

where $c_k = (\min\{k_1, k_2\})^{-1/2}$.

Proof. According to the definition

$$\|q\|_B^2 = (Bq, q) = -(DKGq, q) = (KGq, Gq) \geq \min\{k_1, k_2\}(Gq, Gq) = \min\{k_1, k_2\}\|Gq\|^2,$$

from where follows an estimate (16).

□

Lemma 3.
For any two grid functions g and q, defined on grids ω_u and ω_p, respectively, such that $g = Gq$, following estimate is valid

$$\|g\|_{A^{-1}} \leq c_\nu \|q\|. \tag{17}$$

Proof. According to the definition we have

$$\|g\|_{A^{-1}} = \sup_{\chi \in H_{\omega_u},\ \|\chi\|_A \neq 0} \frac{|(g, \chi)|}{\|\chi\|_A}. \tag{18}$$

Now, using adjoincy of operators D and G and taking into account inequality (15), we obtain

$$|(g, \chi)| = |(Gq, \chi)| = |-(q, D\chi)| \leq \|q\|\|D\chi\| \leq c_\nu \|q\|\|\chi\|_A.$$

Substituting this estimate to the inequality (18), we obtain (17). □

Lemma 4.
For any two grid functions g and q, defined on grids ω_u and ω_p, respectively, such that $q = Dg$, following estimate is valid

$$\|q\|_{B^{-1}} \leq c_\nu \|g\|. \tag{19}$$

Proof. According to the definition we have

$$\|q\|_{B^{-1}} = \sup_{\chi \in H_{\omega_p},\ \|\chi\|_B \neq 0} \frac{|(q,\chi)|}{\|\chi\|_B}. \tag{20}$$

Now using adjoincy of operators D and G and taking into account inequality (19), we obtain

$$|(q,\chi)| = |(Dg,\chi)| = |-(g,G\chi)| \leq \|g\|\|G\chi\| \leq c_k\|g\|\|\chi\|_B.$$

Substituting this estimate to the inequality (20), we obtain (16). □

According to the operator notations introduced above, we can write difference scheme (10) in the operator form

$$\begin{aligned} &Au^{j+1} + Gp^{j+1} = 0,\ \ j = 0, 1, \dots, M-1, \\ &\left(Qp^j + Du^j\right)_t + Bp^j_\sigma = f^j_\sigma,\ \ j = 0, 1, \dots, M-1, \\ &p_0^{j+1} = 0,\ \ u_N^{j+1} = 0,\ \ \ j = 0, 1, \dots, M-1, \\ &Qp^0 + Du^0 = \tfrac{1}{\nu},\ \ \ j = 0. \end{aligned} \tag{21}$$

In the case of continuous coefficients in (2) - (6) (single layered porous media), second order convergence in operator norms is proven in [5]. In this paper we represent theoretical analysis of (21) in the case of discontinuous coefficients.

3.3 Theoretical analysis of the HA scheme

For the proof of convergence of the finite difference scheme we will need a proposition, which is a straightforward reformulation of the similar proposition from [5]:

Proposition 1.

If $\sigma \geq 0.5$, then solution of the difference scheme (21) satisfies following a priori estimate

$$\|u^{j+1}\|^2_A + \|p^{j+1}\|^2_Q \leq \|u^j\|^2_A + \|p^j\|^2_Q + \frac{\tau}{2}\|f^{j+1}_\sigma\|^2_{B^{-1}}. \tag{22}$$

Note that no convergence results for pressure are obtained for the case of incompressible fluid, when compressibility of the fluid $\beta = 0$, and as a result a_1 and a_2 are zero and matrix Q is a zero matrix. To prove convergence, we consider displacement and pressure errors, $z^{u,j}(x) = u^j(x) - u(x,t_j)$ and $z^{p,j}(x) = p^j(x) - p(x,t_j)$, respectively. These errors satisfy the following difference problem

$$\begin{gathered} Az^{u,j+1} + Gz^{p,j+1} = \psi_1^{j+1},\ \ j = 0, 1, ..., M-1, \\ \left(Qz^{p,j} + Dz^{u,j}\right)_t + Bz^{p,j+1}_\sigma = \psi_2^{j+1},\ \ j = 0, 1, ..., M-1, \\ z_0^{p,j+1} = 0,\ \ z_N^{u,j+1} = 0. \end{gathered} \tag{23}$$

Right-hand terms of equations (23), ψ_1^{j+1} and ψ_2^{j+1}, defined on the grids ω_u and ω_p respectively are approximation errors for the first and for the second equations.

3.3.1 Convergence of the scheme in the case of arbitrary location of the interface position

In this subsection we prove convergence result, which is valid for arbitrary location of the interface position with respect to grid points. In other words, parameter θ in the representation (9) can be any value between 0 and 1.
To prove convergence of the scheme, we have to obtain order estimates for errors z^u and z^p, introduced above.
First of all, we split displacement error z^u in the following way

$$z^u = z_1^u + z_2^u, \tag{24}$$

where z_1^u satisfies the problem

$$Az_1^u = \psi_1.$$

¿From this equation one can obtain

$$\|z_1^u\|_A = ||\psi_1||_{A^{-1}}. \tag{25}$$

The approximation error ψ_1 can be represented in a form

$$\psi_{1,i} = (G\eta_1)_i,$$

where η_1 is a function defined on the grid ω_p and $\eta_{1,i} = (\nu_i u_{\bar{x},i+1} - p_i) - (\nu \frac{\partial u}{\partial x} - p)_i$.
Now, the following estimate follows from Lemma 3:

$$\|\psi_1\|_{A^{-1}} \leq c_\nu \|\eta_1\|. \tag{26}$$

Since $\eta_{1,i} = O(h^2)$ for all $i \neq n$, and since $\eta_{1,n} = O(h)$, we obtain $\|\eta_1\| = O(h^{3/2})$. Hence, from the last inequality it follows that

$$\|\psi_1\|_{A^{-1}} = O(h^{3/2}), \tag{27}$$

and from (25)

$$\|z_1^u\|_A = O(h^{3/2}). \tag{28}$$

Consider now the problem for z^p and z_2^u

$$\begin{aligned} Az_2^{u,j+1} + Gz^{p,j+1} = 0 \ , \ \ j = 0, 1, ..., M-1, \\ \left(Qz^{p,j} + Dz_2^{u,j}\right)_t + Bz_\sigma^{p,j+1} = \psi_2^{j+1} - Dz_{1,t}^{u,j} \ , \ \ j = 0, 1, ..., M-1 \end{aligned} \tag{29}$$

If $\sigma \geq 0.5$, it follows from (22):

$$\|z_2^{u,j+1}\|_A^2 + \|z^{p,j+1}\|_Q^2 \leq \|z_2^{u,0}\|_A^2 + \|z^{p,0}\|_Q^2 + \frac{\tau}{2}\sum_{k=0}^{j}\left(\|\psi_2^{k+1}\|_{B^{-1}}^2 + \|Dz_{1_t}^{u,k}\|_{B^{-1}}^2\right), \quad j = 0, \ldots, M-1. \tag{30}$$

First, consider approximation error ψ_2. It can be written in the form

$$\psi_2 = \tilde{\psi}_2 + \tilde{\tilde{\psi}}_2,$$

where

$$\tilde{\psi}_{2,i} = D\eta_{2,i}.$$

Here function η_2 is defined on the grid ω_u,

$$\eta_{2,i} = (k_i p^{\sigma}_{\bar{x},i} - u_{t,i}) - \left(k\frac{\partial p}{\partial x} - \frac{\partial u}{\partial t}\right)|_{x=x_{i-0.5},t=t_{j+0.5}}.$$

If $\theta \leq 0.5$, then

$$\eta_{2,i} = O(h^2 + \tau^{m_\sigma}) \;\; \text{for} \;\; i \neq n,$$
$$\eta_{2,i} = O(h + \tau^{m_\sigma}) \;\; \text{for} \;\; i = n,$$

if $\theta > 0.5$ then

$$\eta_{2,i} = O(h^2 + \tau^{m_\sigma}) \;\; \text{for} \;\; i \neq n+1,$$
$$\eta_{2,i} = O(h + \tau^{m_\sigma}) \;\; \text{for} \;\; i = n+1,$$

where $m_\sigma = 1$ if $\sigma \neq 0.5$ and $m_\sigma = 2$ if $\sigma = 0.5$.
Furthermore, $\tilde{\tilde{\psi}}$ is defined as

$$\tilde{\tilde{\psi}}_{2,i} = \left((ap)_{t,i} - \frac{\partial}{\partial t}(ap)|_{x=x_i,t=t_{j+0.5}}\right) - (\phi^{\sigma}_i - f(x_{i-0.5}, t_{j+0.5})) = O(h^2 + \tau^{m_\sigma}).$$

Applying Lemma 4 and the estimate $\|\tilde{\tilde{\psi}}_2\| \leq c_A\|\tilde{\tilde{\psi}}_2\|_A$ (see, e.g. [10]) with c_A independent on discretization parameters, one can show that the following estimate is valid

$$\|\psi_2\|_{B^{-1}} \leq c_k\|\eta_2\| + c_A\|\tilde{\tilde{\psi}}_2\|. \tag{31}$$

Now, taking into account the orders of approximation of η_2 and $\tilde{\tilde{\psi}}_2$, from (31) we obtain

$$\|\psi_2\|_{B^{-1}} = O(\tau^{m_\sigma} + h^{3/2}). \tag{32}$$

To estimate $\|Dz^u_{1,t}\|_{B^{-1}}$, we apply consequently Lemma 4 and Lemma 1. It gives:

$$\|Dz^u_{1,t}\|_{B^{-1}} \leq c_k c_\nu \|z^u_{1,t}\|_A,$$

Now we recall that (25) is valid, and hence

$$\|Dw_{1,t}\|_{B^{-1}} \leq c_k c_\nu ||\psi_1\|_{A^{-1}}. \tag{33}$$

Now we substitute (33) into (30) and obtain

$$\|z^{u,j+1}_2\|^2_A + \|z^{p,j+1}\|^2_Q \leq \|z^{u,0}_2\|^2_A + \|z^{p,0}\|^2_Q + \frac{\tau}{2}\sum_{k=0}^{j}\left(\|\psi^{k+1}_2\|^2_{B^{-1}} + c_k c_\nu \sum_{k=0}^{j}\|\psi^k_{1_t}\|^2_{A^{-1}}\right), \tag{34}$$

and since (27) and (32) are valid, from (34) we conclude that $\|z^u\|_A + \|z^p\|_Q = O(h^{3/2} + \tau^{m_\sigma})$ or $\|z^u\|_A = O(h^{3/2} + \tau^{m_\sigma})$ and $\|z^p\|_Q = O(h^{3/2} + \tau^{m_\sigma})$. Since the operator Q has a diagonal matrix, it follows $\|z^p\| = O(h^{3/2} + \tau^{m_\sigma})$. Furthermore, since (28) is valid, we have $\|z^u\|_A \leq \|z^u_1\|_A + \|z^u_2\|_A = O(h^{3/2} + \tau^{m_\sigma})$. So, we proved convergence of the pressure in the discrete L_2-norm and convergence of the displacement in A-norm.

3.3.2 Convergence of the scheme in the case when interface position coincides with a node of the grid ω_u

Results proved in the previous subsection are valid for arbitrary interface position, independently of its location with respect to grid points. A better estimate can be obtained in the particular case when the interface coincides with a node of the grid ω_u, i.e. $\zeta = \xi_n$ and θ, defined in (9), is zero. Consider approximation error of the first equation of the system. As it has been shown above,

$$\psi_{1,i} = (G\eta_1)_i, \ \|\psi_1\|_{A^{-1}} \le c_1\|\eta_1\|,$$

where

$$\eta_{1,i} = (\nu_i u_{\bar{x},i+1} - p_i) - \left(\nu\frac{\partial u}{\partial x} - p\right)_i.$$

In the case $\theta = 0$ we have $\eta_{1,i} = O(h^2)$ for all i and hence $\|\eta_1\| = O(h^2)$, and we conclude that $\|\psi_1\|_{A^{-1}} = O(h^2)$. Then for the first part of the displacement error, we obtain the following estimate

$$\|z_1^u\|_A = ||\psi_1\|_{A^{-1}} = O(h^2).$$

Consider now approximation error ψ_2 and recall that it can be splitted in the following way

$$\psi_2 = \tilde{\psi}_2 + \tilde{\tilde{\psi}}_2,$$

with

$$\tilde{\psi}_{2,i} = (D\eta_2)_i, \ \eta_{2,i} = (k_i p^\sigma_{\bar{x},i} - u_{t,i}) - \left(k\frac{\partial p}{\partial x} - \frac{\partial u}{\partial t}\right)|_{x=x_{i-0.5},t=t_{j+0.5}}.$$

and

$$\tilde{\tilde{\psi}}_{2,i} = \left((ap)_t - \frac{\partial}{\partial t}(ap)\right)_i - (f^\sigma - f(x_i, t_{j+0.5})).$$

Let us decouple problem (29). Since operator $A = -GND$, from the first equation we have

$$Dz_2^u = N^{-1}z^p.$$

After substitution Dz_2^u into the second equation of (29) we obtain a problem for the pressure error only:

$$(Q + N^{-1})z_t^p + Bz_\sigma^p = \psi_2 - Dz_{1,t}^u. \tag{35}$$

One should note that $Q + N^{-1}$ is an operator with a positive diagonal matrix.
Now we split the pressure error $z^p = z_1^p + z_2^p$, where z_1^p and z_2^p are solutions of the following problems, respectively

$$(Q + N^{-1})z_{1,t}^p + Bz_{1,\sigma}^p = \psi_2^{**} - Dz_{1,t}^u, \tag{36}$$

$$(Q + N^{-1})z_{2,t}^p + Bz_{2,\sigma}^p = \psi_2^*. \tag{37}$$

Right hand side of the equation (35) was splitted in the following way

$$\psi_2 - Dz_{1,t}^u = \left(\psi_2^{**} - Dz_{1,t}^u\right) + \psi_2^*,$$

where

$$\psi_{2,i}^* = \tilde{\psi}_2(\delta_{k,n-1} + \delta_{k,n})$$

and

$$\psi^{**}_{2,i} = O(h^2 + \tau^{m_\sigma}) \text{ for all } i.$$

For $\sigma \geq 0.5$ solution of the problem (36) can be estimated as (see, e.g. [9])

$$\|z_1^{p,j+1}\| \leq \|z_1^{p,0}\| + \sum_{j'=1}^{j} \tau\|\psi_2^{**j'} - Dz_1^{u,j'}\| \leq \|z_1^{p,0}\| + \tau \sum_{j'=1}^{j} \left(\|\psi_2^{**j'}\| + \|Dz_{1,t}^{u,j'}\|\right). \tag{38}$$

Using Lemma 1 to estimate $Dz_{1,t}^u$, and the fact that $\|z_1^u\|_A = O(h^2)$, from (38) we have $\|z_1^{p,j+1}\| = O(h^2 + \tau^{m_\sigma})$.

Consider now problem (37). Right hand side of this problem can always be represented as

$$\psi^*_{2,k} = (\eta^*_2)_{x,k},$$

where function η^*_2 is defined on the grid $\overline{\omega}_u$ and

$$\eta^*_{2,1} = 0, \ \eta^*_{2,i} = \sum_{s=1}^{i-1} h\psi^*_{2,s}, \ i = 2, \ldots, N.$$

Using identity $z_2^{p,\sigma} = z_2^p + \sigma\tau z_{2,t}^p$, and then applying the operator B^{-1} to (37), we can rewrite this problem as

$$\left(B^{-1}(Q + N^{-1}) + \sigma\tau E\right) z_{2,t}^p + z_2^p = B^{-1}\psi^*_2. \tag{39}$$

Operators B^{-1} and N^{-1} are positive definite ones, operator Q is non negative, hence $B^{-1}(Q+N^{-1})$ is positive definite, and for $\sigma \geq 0.5$ the following inequality holds

$$B^{-1}(Q + N^{-1}) + \sigma\tau E \geq \frac{\tau}{2}E.$$

In this case we can write an estimate (see, e.g. [9]) for the solution of the problem (39):

$$\|z_2^{p,j+1}\| \leq \|B^{-1}\psi_2^{*0}\| + \|B^{-1}\psi_2^{*j}\| + \sum_{j'=1}^{j} \tau\|B^{-1}\psi_{2,\bar{t}}^{*j'}\|. \tag{40}$$

Here $\|B^{-1}\psi_2^{*j}\|$ can be estimated as (see [9])

$$\|B^{-1}\psi_2^{*j}\| \leq c(1, |\eta^*_2|)_{\overline{\omega}_u}, \tag{41}$$

where c is some constant independent on discretization parameters. Now we have to estimate $(1, |\eta^*_2|)_{\overline{\omega}_u}$. According to the definition of η^*_2 we can write

$$(1, |\eta^*_2|)_{\overline{\omega}_u} = \sum_{i=n-1}^{N} h|\eta^*_{2,i}| = h^2|\psi^*_{2,n-1}| + h|\psi^*_{2,n-1} + \psi^*_{2,n}|.$$

Recall that $\psi^*_{2,i} = \tilde{\psi}_2(\delta_{i,n-1} + \delta_{i,n})$ and one can show that

$$\tilde{\psi}_{2,i} = (D\eta_2)_i = \begin{cases} O(h^2 + \tau^{m_\sigma}) & \text{for } \ i \neq n-1, n \\ \frac{\eta_{2,n}}{h} + O(h + \tau^{m_\sigma}) & \text{for } \ i = n-1, \\ -\frac{\eta_{2,n}}{h} + O(h + \tau^{m_\sigma}) & \text{for } \ i = n, \end{cases}$$

where $\eta_{2,n} = O(h)$. It follows from last formulas that

$$\psi^*_{2,n-1} = O(h^0 + \tau^{m_\sigma})$$

$$\psi^*_{2,n} = O(h^0 + \tau^{m_\sigma})$$

$$\psi^*_{2,n-1} + \psi^*_{2,n} = O(h + \tau^{m_\sigma})$$

Substituting these expressions into the formula for $(1, |\eta^*_2|)_{\overline{\omega}_u}$, we see that $(1, |\eta^*_2|)_{\overline{\omega}_u} = O(h^2+\tau^{m_\sigma})$. Now from (41) we can conclude that $\|B^{-1}\psi^*_2\| = O(h^2 + \tau^{m_\sigma})$. Furthermore, it follows from (40):

$$\|z_2^{p,j+1}\| = O(h^2 + \tau^{m_\sigma}).$$

Finally, we can estimate pressure error

$$\|z^p\| \le \|z^p_1\| + \|z^p_2\| = O(h^2 + \tau^{m_\sigma}).$$

To complete the estimate, it remains to estimate $\|z^u_2\|_A$. Multiplying first equation of (29) by z^u_2, we obtain:

$$\|z^u_2\|^2_A = -(Gz^p, z^u_2).$$

Taking into account that $(Gz^p, z^u_2) = -(z^p, Dz^u_2)$ and then applying ϵ-inequality, we have

$$\|z^u_2\|^2_A \le \epsilon\|z^p\|^2 + \frac{1}{4\epsilon}\|Dz^u_2\|^2.$$

Now, according to the Lemma 1, we can write

$$\|z^u_2\|^2_A \le \epsilon\|z^p\|^2 + \frac{c^2_\nu}{4\epsilon}\|z^u_2\|^2_A.$$

We choose ϵ in such a way that $1 - \frac{c^2_\nu}{4\epsilon} > 0$, and from the previous inequality we obtain the following estimate

$$\|z^u_2\|_A \le \sqrt{\frac{\epsilon}{1 - \frac{c^2_\nu}{4\epsilon}}}\|z^p\|.$$

¿From here we conclude that $\|z^u_2\|_A = O(h^2 + \tau^{m_\sigma})$. And finally, we are able to estimate the whole displacement error

$$\|z^u\|_A \le \|z^u_1\|_A + \|z^u_2\|_A = O(h^2 + \tau^{m_\sigma}).$$

Thus, second order convergence of displacement and pressure was proved for the particular case, when interface position coincide with a grid node of ω_u.

4 Modified finite volume approximations

Scheme (10) gives us first order of approximation for both fluxes: $W(x,t) = -\nu\frac{\partial u}{\partial x}$ and $V(x,t) = -k\frac{\partial p}{\partial x}$, what means first order of approximation for the stress of the solid and for the velocity of the fluid.

Now we will derive two modifications of the scheme, which will allow us to achieve second order of approximation for the stress and for the velocity.

Remind, that flux $W(x,t)$ in the scheme (10) is approximated in the grid points $\overline{\omega}_p$ and flux $V(x,t)$ - in the grid points $\overline{\omega}_u$. Respective expressions are

$$w_i = w(x_i) = \begin{cases} 0, & i = 0, \\ -(\nu_i u_{\overline{x},i+1}), & i = 1, 2, \ldots, N-2, \\ -\nu_{N-1}\frac{u_{N-1}}{h}, & i = N-1, \end{cases} \tag{42}$$

$$v_i = v(\xi_i) = \begin{cases} k_1\frac{p_1}{h}, & i = 1, \\ -(kp_{\overline{x},i})_i, & i = 2, 3, \ldots, N-1, \\ 0, & i = N. \end{cases} \tag{43}$$

where

$$\nu_i = \left(\frac{1}{h}\int\limits_{\xi_i}^{\xi_{i+1}} \frac{dx}{\nu(x)}\right)^{-1}, \quad k_i = \left(\frac{1}{h}\int\limits_{x_{i-1}}^{x_i} \frac{dx}{k(x)}\right)^{-1}, \tag{44}$$

are harmonic averages of coefficients $\nu(x)$ and $k(x)$.
Using notations (42) and (43), finite-difference scheme (10) can be rewritten in the following form

$$\text{for } j = 0, \ldots, M-1$$

$$w_0^j = 0,\ p_0^j = 0, \tag{45}$$

$$w_{x,i-1}^j + p_{\overline{x},i}^j = 0,\ i = 1, \ldots, N-1, \tag{46}$$

$$(a_i p_i^j + u_{x,i}^j)_t + v_{x,i}^j = \phi_i^\sigma,\ i = 1, \ldots, N-1, \tag{47}$$

$$w_N^j = 0,\ u_N^j = 0, \tag{48}$$

$$a_i p_i^0 + u_{x,i}^0 = \frac{1}{\nu_i^h}, \quad i = 1, \ldots, N-1, \quad j = 0, \tag{49}$$

4.1 Finite difference scheme with improved approximation of the stress

Suppose now that interface position coincides with one of the points ω_p, i.e. $\zeta = x_n$, $1 \le n \le N-1$, $x_n \in \omega_p$. Consider harmonic averaging of the flux $W(x,t)$ in the interface point x_n

$$w_n = \nu_n \frac{u_{n+1} - u_n}{h}$$

and expand u_n and u_{n+1} around the interface point:

$$u_n = u(\zeta - 0, t) - \frac{h}{2}\left(\frac{\partial u}{\partial x}\right)^- + \frac{h^2}{8}\left(\frac{\partial^2 u}{\partial x^2}\right)^- - \frac{h^3}{48}\left(\frac{\partial^3 u}{\partial x^3}\right)^- + O(h^4), \tag{50}$$

$$u_{n+1} = u(\zeta + 0, t) + \frac{h}{2}\left(\frac{\partial u}{\partial x}\right)^+ + \frac{h^2}{8}\left(\frac{\partial^2 u}{\partial x^2}\right)^+ + \frac{h^3}{48}\left(\frac{\partial^3 u}{\partial x^3}\right)^+ + O(h^4), \tag{51}$$

where we designated $\left(\frac{\partial^k u}{\partial x^k}\right)^- = \frac{\partial^k u}{\partial x^k}(\zeta - 0, t)$ and $\left(\frac{\partial^k u}{\partial x^k}\right)^+ = \frac{\partial^k u}{\partial x^k}(\zeta + 0, t)$.

Now we substitute expansions (50) and (51) into the expression for w_n and recall that $u(\zeta - 0, t) = u(\zeta + 0, t)$. Then we have

$$
\begin{aligned}
w_n = -\nu_n^h \frac{u_{n+1} - u_n}{h} = -\frac{2\nu_1\nu_2}{\nu_1+\nu_2}\frac{u_{n+1} - u_n}{h} = \\
-\frac{1}{\nu_1+\nu_2}\left(\nu_2\nu_1\left(\frac{\partial u}{\partial x}\right)^- + \nu_1\nu_2\left(\frac{\partial u}{\partial x}\right)^+\right) - \\
\frac{h}{4(\nu_1+\nu_2)}\left(\nu_1\frac{\partial}{\partial x}\left(\nu_2\left(\frac{\partial u}{\partial x}\right)^+\right) - \nu_2\frac{\partial}{\partial x}\left(\nu_1\left(\frac{\partial u}{\partial x}\right)^-\right)\right) - \\
\frac{h^2}{24(\nu_1+\nu_2)}\left(\nu_1\frac{\partial^2}{\partial x^2}\left(\nu_2\left(\frac{\partial u}{\partial x}\right)^+\right) + \nu_2\frac{\partial^2}{\partial x^2}\left(\nu_1\left(\frac{\partial u}{\partial x}\right)^-\right)\right).
\end{aligned}
\tag{52}
$$

Now we account for the stress continuity condition across the interface

$$
\nu_1\left(\frac{\partial u}{\partial x}\right)^- = \nu_2\left(\frac{\partial u}{\partial x}\right)^+
$$

and rewrite (52) as

$$
\begin{aligned}
w_n = -\nu_1\left(\frac{\partial u}{\partial x}\right)^- - \frac{h}{4(\nu_1+\nu_2)}\left(\nu_2\frac{\partial}{\partial x}\left(\nu_1\left(\frac{\partial u}{\partial x}\right)^-\right) - \nu_1\frac{\partial}{\partial x}\left(\nu_2\left(\frac{\partial u}{\partial x}\right)^+\right)\right) + O(h^2) = \\
= W(x_n,t) - \frac{h}{4(\nu_1+\nu_2)}\left(\nu_2\frac{\partial W_n^-}{\partial x} - \nu_1\frac{\partial W_n^+}{\partial x}\right) + O(h^2).
\end{aligned}
$$

¿From here we can find modified approximation expression for the flux $W(x_n, t)$:

$$
\tilde{w}_n = -\nu_n^h u_{\overline{x},n+1} - \frac{h}{4}\frac{\nu_1\frac{\partial W_n^+}{\partial x} - \nu_2\frac{\partial W_n^-}{\partial x}}{\nu_1+\nu_2}. \tag{53}
$$

Note that according to this derivation $\tilde{w}_n = W(x_n, t) + O(h^2)$.
Suppose that the first equation of (7) is valid on the interface, and hence we can express

$$
\frac{\partial W_n^-}{\partial x} = -\left(\frac{\partial p}{\partial x}\right)^-,
$$

$$
\frac{\partial W_n^+}{\partial x} = -\left(\frac{\partial p}{\partial x}\right)^+
$$

and rewrite expression (53)

$$
\tilde{w}_n = -\nu_n^h u_{\overline{x},n+1} + \frac{h}{4}\frac{\nu_1\left(\frac{\partial p}{\partial x}\right)^+ - \nu_2\left(\frac{\partial p}{\partial x}\right)^-}{\nu_1+\nu_2}. \tag{54}
$$

Using interface continuity condition for fluid velocity

$$k_1 \left(\frac{\partial p}{\partial x}\right)^- = k_2 \left(\frac{\partial p}{\partial x}\right)^+,$$

and approximating derivatives $\left(\frac{\partial p}{\partial x}\right)^-$ and $\left(\frac{\partial p}{\partial x}\right)^+$ by difference expressions $p_{\overline{x},n}$ and $p_{\overline{x},n+1}$, respectively, we obtain the following approximations of the flux

$$\tilde{w}_n^1 = -\nu_n^h u_{\overline{x},n+1} + \frac{h}{4}\frac{\nu_1 \frac{k_1}{k_2} - \nu_2}{\nu_1 + \nu_2} p_{\overline{x},n} \tag{55}$$

or

$$\tilde{w}_n^2 = -\nu_n^h u_{\overline{x},n+1} + \frac{h}{4}\frac{\nu_1 - \nu_2 \frac{k_2}{k_1}}{\nu_1 + \nu_2} p_{\overline{x},n+1}. \tag{56}$$

Note that $\tilde{w}_n^1 = W(x_n, t) + O(h^2)$ and $\tilde{w}_n^2 = W(x_n, t) + O(h^2)$. According to the modification of the flux approximation, we modify two equations of (46) - for $i = n$ and for $i = n + 1$:

$$-(\nu_1 u_{\overline{x}})_{x,n} + \left(\frac{1}{4}\frac{\nu_1 \frac{k_1}{k_2} - \nu_2}{\nu_1 + \nu_2} + 1\right) p_{\overline{x},n} = 0, \ i = n \tag{57}$$

and

$$-(\nu_2 u_{\overline{x}})_{x,n+1} + \left(1 - \frac{1}{4}\frac{\nu_1 - \nu_2 \frac{k_2}{k_1}}{\nu_1 + \nu_2}\right) p_{\overline{x},n+1} = 0, \ i = n + 1. \tag{58}$$

So, difference between modified scheme and scheme (45) - (49) consists in approximation of the flux $W(x, t)$ in the point x_n, and as a consequence in approximation of the first equation of the system (7) in two neighboring to the interface points, ξ_n and ξ_{n+1}. Modified scheme provides second order of approximation both for stress and velocity when the interface position coincides with point x_n.
Note that modifications performed above give no improvement in case when parameters of the media are such that $\nu_1 k_1 = \nu_2 k_2$, and it gives negligibly small improvement when following inequalities take place:

$$\left|\frac{1}{4}\frac{\nu_1 \frac{k_1}{k_2} - \nu_2}{\nu_1 + \nu_2}\right| << 1, \tag{59}$$

$$\left|\frac{1}{4}\frac{\nu_1 - \nu_2 \frac{k_2}{k_1}}{\nu_1 + \nu_2}\right| << 1. \tag{60}$$

One can easily see it from modified expressions for fluxes (55), (56) and from modified equations (57), (58) - the corresponding correcting items in these formulas will be negligibly small.

4.2 Finite difference scheme with improved approximation of the velocity

Let us derive now another modification of the scheme (45) - (49). Suppose that interface position coincides now with one of the points of the grid $\overline{\omega}_u$, i.e. $\zeta = \xi_n$, where $1 \leq n \leq N-1$ is some integer. Analogously to the previous case we derive modified expression, approximating another flux $V(x,t)$ with the second order

$$\tilde{v}_n = -k_n^h p_{\overline{x},n} - \frac{h}{4}\frac{k_1\left(\frac{\partial V}{\partial x}\right)_n^+ - k_2\left(\frac{\partial V}{\partial x}\right)_n^-}{k_1+k_2}. \tag{61}$$

Suppose now that the second equation of the system (7) is valid on the interface, then we can express

$$\left(\frac{\partial V}{\partial x}\right)_n^- = \left(f - \frac{\partial}{\partial t}\left(a_1 p + \frac{\partial u}{\partial x}\right)\right)_n^-,$$

$$\left(\frac{\partial V}{\partial x}\right)_n^+ = \left(f - \frac{\partial}{\partial t}\left(a_2 p + \frac{\partial u}{\partial x}\right)\right)_n^+$$

and rewrite expression (62)

$$\tilde{v}_n = -k_n^h p_{\overline{x},n} - \frac{h}{4}\frac{k_1\left(f - \frac{\partial}{\partial t}\left(a_2 p + \frac{\partial u}{\partial x}\right)\right)_n^+ - k_2\left(f - \frac{\partial}{\partial t}\left(a_1 p + \frac{\partial u}{\partial x}\right)\right)_n^-}{k_1+k_2}.$$

Using interface condition

$$\nu_1\left(\frac{\partial u}{\partial x}\right)^- = \nu_2\left(\frac{\partial u}{\partial x}\right)^+,$$

and approximating continuous derivatives $\left(\frac{\partial u}{\partial x}\right)^-$ and $\left(\frac{\partial u}{\partial x}\right)^+$ with difference derivatives $u_{x,n-1}$ and $u_{x,n}$, respectively, we obtain following expressions for the flux $V(\xi_n,t)$

$$\tilde{v}_n^1 = -k_n^h p_{\overline{x},n} - \frac{h}{4}\frac{k_1 f_n^+ - k_2 f_n^-}{k_1+k_2} - \frac{h}{4}\frac{k_2\left(a_1 p_{n-1} + u_{x,n-1}\right)_t - k_1\left(a_2 p_{n-1} + \frac{\nu_1}{\nu_2}u_{x,n-1}\right)_t}{k_1+k_2} \tag{62}$$

or

$$\tilde{v}_n^2 = -k_n^h p_{\overline{x},n} - \frac{h}{4}\frac{k_1 f_n^+ - k_2 f_n^-}{k_1+k_2} - \frac{h}{4}\frac{k_2\left(a_1 p_n + \frac{\nu_2}{\nu_1}u_{x,n}\right)_t - k_1\left(a_2 p_n + u_{x,n}\right)_t}{k_1+k_2}. \tag{63}$$

Note that according to the derivation $\tilde{v}_n^1 = V(\xi_n,t) + O(h^2)$ and $\tilde{v}_n^2 = V(\xi_n,t)+O(h^2)$. According to the modification of the flux we should also modify two equations of (47) - for $i = n-1$ and $i = n$:

$$\left(\left(a_1 + \frac{1}{4}\frac{k_1 a_2 - k_2 a_1}{k_1+k_2}\right)p_{n-1} + \left(1 + \frac{1}{4}\frac{k_1\frac{\nu_1}{\nu_2} - k_2}{k_1+k_2}\right)u_{x,n-1}\right)_t - (k_1 p_{\overline{x}})_{x,n-1} = f_{n-1} + \frac{1}{4}\frac{k_1 f_n^+ - k_2 f_n^-}{k_1+k_2}, \quad i = n-1, \tag{64}$$

$$\left(\left(a_2+\frac{1}{4}\frac{k_2a_1-k_1a_2}{k_1+k_2}\right)p_n+\left(1+\frac{1}{4}\frac{k_2\frac{\nu_2}{\nu_1}-k_1}{k_1+k_2}\right)u_{x,n}\right)_t-$$
$$(k_2p_{\overline{x}})_{x,n}=f_n-\frac{1}{4}\frac{k_1f_n^+-k_2f_n^-}{k_1+k_2},\quad i=n. \tag{65}$$

Modified in such a way scheme provides second order of approximation both for stress and velocity when the interface position coincides with point ξ_n.
One can easily see from (62), (63) and (64), (65) that modifications performed above can be useless in case when for the certain set of parameters and for the certain discretization following equalities are valid:

$$k_1a_2=k_2a_1,$$
$$k_1\nu_1=k_2\nu_2,$$
$$k_1f_n^+=k_2f_n^-.$$

In this case all correcting items in corresponding expressions turn to zero and obtained scheme is identical to the initial one. One can also note that improvement can be almost inessential when parameters are such that corresponding correcting items in formulas (62), (63) and (64), (65) are very small.

So, two modifications of the scheme (45) - (49) were obtained above, and both of them under the certain condition for the interface location with respect to the grid points, give second order of approximation for stress and velocity.

4.3 Theoretical analysis of a modified scheme

Let us write the scheme (45) - (49) with modifications (64) and (65) in the operator form:

$$\begin{aligned}
&Au^{j+1}+Gp^{j+1}=0,\ j=0,1,\dots,M-1,\\
&\left(\tilde{Q}p^j+RDu^j\right)_t+Bp^j_\sigma=\tilde{f}^j_\sigma,\ \ j=0,1,\dots,M-1,\\
&p_0^{j+1}=0,\ u_N^{j+1}=0,\ \ j=0,1,\dots,M-1,\\
&Qp^0+Du^0=\tfrac{1}{\nu},\ \ j=0,
\end{aligned} \tag{66}$$

where operators A, G, B and D were introduced above, and $\tilde{Q}:H_{\omega_p}\to H_{\omega_p}$ and $R:H_{\omega_p}\to H_{\omega_p}$ are constant operators defined by the following formulae

$$(\tilde{Q}p)_i=\begin{cases} a_1p_i, & \text{for } i=1,\dots,n-2,\\ \left(a_1+\frac{k_1a_2-k_2a_1}{k_1+k_2}\right)p_i, & \text{for } i=n-1,\\ \left(a_2-\frac{k_1a_2-k_2a_1}{k_1+k_2}\right)p_i, & \text{for } i=n,\\ a_2p_i, & \text{for } i=n+1,\dots,N-1,\end{cases} \tag{67}$$

$$(Rq)_i = \begin{cases} q_i, & \text{for } i = 1, \ldots, n-2, \\ \left(1 + \frac{1}{4}\frac{k_1\frac{\nu_1}{\nu_2} - k_2}{k_1 + k_2}\right) q_i, & \text{for } i = n-1, \\ \left(1 + \frac{1}{4}\frac{k_2\frac{\nu_2}{\nu_1} - k_1}{k_1 + k_2}\right) q_i, & \text{for } i = n, \\ q_i, & \text{for } i = n+1, \ldots, N-1, \end{cases} \tag{68}$$

and modified right hand side $\tilde{f}$ is

$$\tilde{f}_i = \begin{cases} f_i, & \text{for } i \neq n-1, n, \\ f_i + \frac{1}{4}\frac{k_1 f_n^+ - k_2 f_n^-}{k_1 + k_2}, & \text{for } i = n-1, \\ f_i - \frac{1}{4}\frac{k_1 f_n^+ - k_2 f_n^-}{k_1 + k_2}, & \text{for } i = n. \end{cases} \tag{69}$$

Now we multiply second equation of (66) by R^{-1} and, designating $\tilde{\tilde{Q}} = R^{-1}\tilde{Q}$, it as

$$\left(\tilde{\tilde{Q}} p^j + Du^j\right)_t + R^{-1}Bp^j_\sigma = R^{-1}\tilde{f}^j_\sigma. \tag{70}$$

Note that operator $\tilde{\tilde{Q}} = R^{-1}\tilde{Q}$ is positive definite and has a diagonal matrix, since both Q and R^{-1} are positive definite operators with diagonal matrices. Operator $R^{-1}B$ is positive definite, but not self-adjoint, since operators R^{-1} and B are not commutative. For our proof we will need a proposition

Proposition 2.

For $\sigma \geq 0.5$ the solution of the difference scheme (66) satisfies following a priori estimate

$$\|u^{j+1}\|^2_A + \|p^{j+1}\|^2_{\tilde{\tilde{Q}}} \leq \|u^j\|^2_A + \|p^j\|^2_{\tilde{\tilde{Q}}} + \frac{r_2^2}{4r_1}\tau\|f^{j+1}_\sigma\|^2_{B^{-1}}, \tag{71}$$

where $r_1 = \max\{r_{ii}\}$ and $r_2 = \min\{r_{ii}\}$.

Proof.

¿From the first equation of (66) we have

$$\left(Au^{j+1}_\sigma, u^j_t\right) + \left(Gp^{j+1}_\sigma, u^j_t\right) = 0, \tag{72}$$

and from the (70)

$$(\tilde{\tilde{Q}} p^j_t, p^{j+1}_\sigma) + (Du^j_t, p^{j+1}_\sigma) + (R^{-1}Bp^j_\sigma, p^{j+1}_\sigma) = (R^{-1}\tilde{f}^j_\sigma, p^{j+1}_\sigma). \tag{73}$$

Now we add (72) and (73) and recall that for operators G and D adjoint condition $(Gp, u)_{\omega_u} = -(p, Du)_{\omega_p}$ is valid, then we obtain

$$(Au^{j+1}_\sigma, u^j_t) + (\tilde{\tilde{Q}} p^j_t, p^{j+1}_\sigma) + (R^{-1}Bp^{j+1}_\sigma, p^{j+1}_\sigma) = (R^{-1}\tilde{f}^{j+1}_\sigma, p^{j+1}_\sigma). \tag{74}$$

Now we make following estimates:

$$(R^{-1}Bp^{j+1}_\sigma, p^{j+1}_\sigma) \geq r_1(Bp_\sigma, p_\sigma) = r_1\|p_\sigma\|^2_B,$$

and

$$(R^{-1}\tilde{f}^j_\sigma, p^{j+1}_\sigma) \le |(R^{-1}\tilde{f}^j_\sigma, p^{j+1}_\sigma)| \le r_2|(\tilde{f}^j_\sigma, p^{j+1}_\sigma)| \le r_2\left(\frac{1}{2\epsilon}\|\tilde{f}^{j+1}_\sigma\|^2_{B^{-1}} + \frac{\epsilon}{2}\|p^{j+1}_\sigma\|^2_B\right).$$

In the second estimate we applied ϵ-inequality with some parameter $\epsilon > 0$.
Now we substitute two previous estimates into the equation (74):

$$(Au^{j+1}_\sigma, u^j_t) + (\tilde{\tilde{Q}}p^j_t, p^{j+1}_\sigma) + r_1\|p_\sigma\|^2_B \le \frac{r_2}{2\epsilon}\|\tilde{f}^{j+1}_\sigma\|^2_{B^{-1}} + \frac{r_2\epsilon}{2}\|p^{j+1}_\sigma\|^2_B. \tag{75}$$

We choose the value of parameter ϵ in a way to cancel items $r_1\|p_\sigma\|^2_B$ and $\frac{r_2\epsilon}{2}\|p^{j+1}_\sigma\|^2_B$ in the previous inequality. It corresponds to $\epsilon = \frac{2r_1}{r_2}$, and then we have:

$$(Au^{j+1}_\sigma, u^j_t) + (\tilde{\tilde{Q}}p^j_t, p^{j+1}_\sigma) \le \frac{r_2^2}{4r_1}\|\tilde{f}^{j+1}_\sigma\|^2_{B^{-1}}.$$

Finally, after substituting here expressions for u^{j+1}_σ, u^j_t and p^{j+1}_σ, and performing some simple calculations, we obtain the estimate (71).

□

Consider now displacement and pressure errors $z^{u,j}(x) = u^j(x) - u(x,t_j)$ and $z^{p,j}(x) = p^j(x) - p(x,t_j)$ respectively. These errors must satisfy following difference problem

$$\begin{gathered} Az^{u,j+1} + Gz^{p,j+1} = \psi^{j+1}_1,\ \ j = 0,1,...,M-1, \\ \left(\tilde{Q}z^{p,j} + RDz^{u,j}\right)_t + Bz^{p,j+1}_\sigma = \psi^{j+1}_2,\ \ j = 0,1,...,M-1, \\ z^{p,j+1}_0 = 0,\ z^{u,j+1}_N = 0. \end{gathered} \tag{76}$$

Consider approximation error of the second equation. It can be represented in the following form:

$$\psi^{j+1}_{2,i} = \left((\tilde{Q}p(x_i,t_j))_t - \frac{1}{h}\int\limits_{\xi_i}^{\xi_{i+1}} \frac{\partial}{\partial t}\left(ap(x,t)\right)dx(t_{j+0.5})\right) - \left(\left(v(\xi_i,t_{j+0.5}) + u_t(\xi_i,t_{j+0.5})\right) - \left(V(\xi_i,t_{j+0.5}) + \frac{\partial u}{\partial t}(\xi_i,t_{j+0.5})\right)\right)_x + \left(f_\sigma(x_i,t_{j+0.5}) - \frac{1}{h}\int\limits_{\xi_i}^{\xi_{i+1}} f(x,t_{j-0.5})dx\right),\ \text{for } i \ne n-1,n, \tag{77}$$

$$\psi^{j+1}_{2,n-1} = \left((\tilde{Q}p(x_{n-1},t_j))_t - \frac{1}{h}\int\limits_{\xi_{n-1}}^{\xi_n} \frac{\partial}{\partial t}\left(ap(x,t)\right)dx(t_{j+0.5})\right) - \left(\left(\frac{\tilde{v}^1_n - v_{n-1}}{h} + u_{xt}(\xi_{n-1},t_{j+0.5})\right) - \left(V(\xi_{n-1},t_{j+0.5}) + \frac{\partial u}{\partial t}(\xi_{n-1},t_{j+0.5})\right)_x\right) + \left(f_\sigma(x_{n-1},t_{j+0.5}) - \frac{1}{h}\int\limits_{\xi_{n-1}}^{\xi_n} f(x,t_{j-0.5})dx\right),\ \text{for } i = n-1, \tag{78}$$

$$\psi_{2,n}^{j+1} = \left((\tilde{Q}p(x_n, t_j))_t - \frac{1}{h} \int\limits_{\xi_n}^{\xi_{n+1}} \frac{\partial}{\partial t} \left(ap(x,t) \right) dx (t_{j+0.5}) \right) -$$

$$\left(\left(\frac{v_{n+1} - \tilde{v}_n^2}{h} + u_{xt}(\xi_n, t_{j+0.5}) \right) - \left(V(\xi_n, t_{j+0.5}) + \frac{\partial u}{\partial t}(\xi_n, t_{j+0.5}) \right)_x \right) +$$

$$\left(f_\sigma(x_n, t_{j+0.5}) - \frac{1}{h} \int\limits_{\xi_n}^{\xi_{n+1}} f(x, t_{j-0.5}) dx \right), \text{ for } i = n, \quad (79)$$

where

$$V(x,t) = k \frac{\partial p}{\partial x},$$

$$v(\xi_i, t_{j-0.5}) = \begin{cases} k(\xi_i, t_{j-0.5}) \frac{p(x_i, t_{j-0.5}) - p(x_{i-1}, t_{j-0.5})}{h}, & i = 1, \ldots, N-1, \\ 0, \quad i = N. \end{cases} \quad (80)$$

and $\tilde{v}_n^1$ and $\tilde{v}_n^2$ are fluxes, calculated by formulae (55) and (56) respectively, using values of exact solutions $p(x, t_{j-0.5})$ and $u(x, t_{j-0.5})$ at respective grid points.
Now we split approximation error $\psi_2 = \psi_2^* + \psi_2^{**}$, where

$$\psi_{2,i}^{**j+1} = \left((\tilde{Q}p(x_i, t_j))_t - \frac{1}{h} \int\limits_{\xi_i}^{\xi_{i+1}} \frac{\partial}{\partial t} \left(ap(x,t) \right) dx (t_{j+0.5}) \right) -$$

$$\left(f_\sigma(x_i, t_{j+0.5}) - \frac{1}{h} \int\limits_{\xi_i}^{\xi_{i+1}} f(x, t_{j-0.5}) dx \right) = O(h^2 + \tau^{m_\sigma}) \text{ for all } i,$$

and

$$\psi_{2,i}^{*j+1} = \left((v(\xi_i, t_{j+0.5}) + u_t(\xi_i, t_{j+0.5})) - \left(V(\xi_i, t_{j+0.5}) + \frac{\partial u}{\partial t}(\xi_i, t_{j+0.5}) \right) \right)_x =$$

$$O(h^2 + \tau^{m_\sigma}) \text{ for all } i \neq n-1, n,$$

$$\psi_{2,n-1}^{*j+1} = \left(\frac{\tilde{v}_n^1 - v_{n-1}}{h} + u_{xt}(\xi_{n-1}, t_{j+0.5}) \right) - \left(V(\xi_{n-1}, t_{j+0.5}) + \frac{\partial u}{\partial t}(\xi_{n-1}, t_{j+0.5}) \right)_x, \quad i = n-1,$$

$$\psi_{2,n}^{*j+1} = \left(\frac{v_{n+1} - \tilde{v}_n^2}{h} + u_{xt}(\xi_n, t_{j+0.5}) \right) - \left(V(\xi_n, t_{j+0.5}) + \frac{\partial u}{\partial t}(\xi_n, t_{j+0.5}) \right)_x, \quad i = n.$$

Now we introduce following grid functions:

$$\eta_i^{j+1} = (v(\xi_i, t_{j+0.5}) + u_t(\xi_i, t_{j+0.5})) - \left(V(\xi_i, t_{j+0.5}) + \frac{\partial u}{\partial t}(\xi_i, t_{j+0.5}) \right), \ i \neq n,$$

$$\tilde{\eta}_n^{1,j+1} = \left(\tilde{v}_n^1 + u_t(\xi_n, t_{j+0.5})\right) - \left(V(\xi_n, t_{j+0.5}) + \frac{\partial u}{\partial t}(\xi_n, t_{j+0.5}) \right),$$

$$\tilde{\eta}_n^{2,j+1} = \left(\tilde{v}_n^2 + u_t(\xi_n, t_{j+0.5})\right) - \left(V(\xi_n, t_{j+0.5}) + \frac{\partial u}{\partial t}(\xi_n, t_{j+0.5}) \right).$$

Note that due to the boundary conditions $\eta_N^{j+1} = 0$.

According to this designation we rewrite ψ_2^* in the following way:

$$\psi_{2,i}^* = \begin{cases} \eta_{x,i}, & i \neq n-1, n, \\ \frac{\tilde{\eta}_n^1 - \eta_{n-1}}{h}, & i = n-1, \\ \frac{\eta_{n+1} - \tilde{\eta}_n^2}{h}, & i = n. \end{cases} \tag{81}$$

Now we want to write ψ_2^* in the divergent form and for this purpose construct a new grid function η^*, defined on the grid $\overline{\omega}_u$:

$$\eta_i^* = \begin{cases} \eta_i + \tilde{\eta}_n^2, & i = 1, \dots, n-1, \\ \tilde{\eta}_n^1 + \tilde{\eta}_n^2, & i = n, \\ \tilde{\eta}_n^1 + \eta_i, & i = n+1, \dots, N. \end{cases} \tag{82}$$

Note that since $\eta_i = O(h^2 + \tau^{m_\sigma})$ for all i, $\tilde{\eta}_n^1 = O(h^2 + \tau^{m_\sigma})$ and $\tilde{\eta}_n^2 = O(h^2 + \tau^{m_\sigma})$, it follows from (82) that $\eta_i^* = O(h^2 + \tau^{m_\sigma})$ for all i.

One can easily see that

$$\psi_{2,i}^* = \eta_{x,i}^*, \ i = 1, \dots, N-1.$$

Note also that $\psi_{2,0}^* = 0$.

Now we need an estimate for the $\|\psi_2^*\|_{B^{-1}}$. According to the definition

$$\|\psi_2^*\|_{B^{-1}} = \sup_{\chi \in H_{\omega_p}, \ \|\chi\|_B \neq 0, \ \chi_0 = 0} \frac{|(\psi_2^*, \chi)|}{\|\chi\|_B}. \tag{83}$$

Now

$$|(\psi_2^*, \chi)| = |(\eta_x^*, \chi)| = |-(\eta^*, \chi_{\overline{x}}) + \eta_N^* \chi_{N-1}| \leq |-(\eta^*, \chi_{\overline{x}})| + |\eta_N^* \chi_{N-1}| \leq$$
$$\leq \|\eta^*\| \|\chi_{\overline{x}}\| + |\eta_N^*| \, |\chi_{N-1}| \leq c_k \|\eta^*\| \|\chi\|_B + |\eta_N^*| \, \|\chi\|_c \leq c_k \|\eta^*\| \|\chi\|_B + \overline{c} \, |\eta_N^*| \, \|\chi\|_B.$$

Substituting this estimate to the (83), we obtain

$$\|\psi_2^*\|_{B^{-1}} \leq c_k \|\eta^*\| + \overline{c} \, |\eta_N^*| \,,$$

and since $\eta_i^* = O(h^2 + \tau^{m_\sigma})$ for all i, we conclude that $\|\psi_2^*\|_{B^{-1}} = O(h^2 + \tau^{m_\sigma})$.

The reminder of the proof is just a straightforward repetition of the end of proof from the subsection 3.3.2 with some modification according to this particular case, which are not .

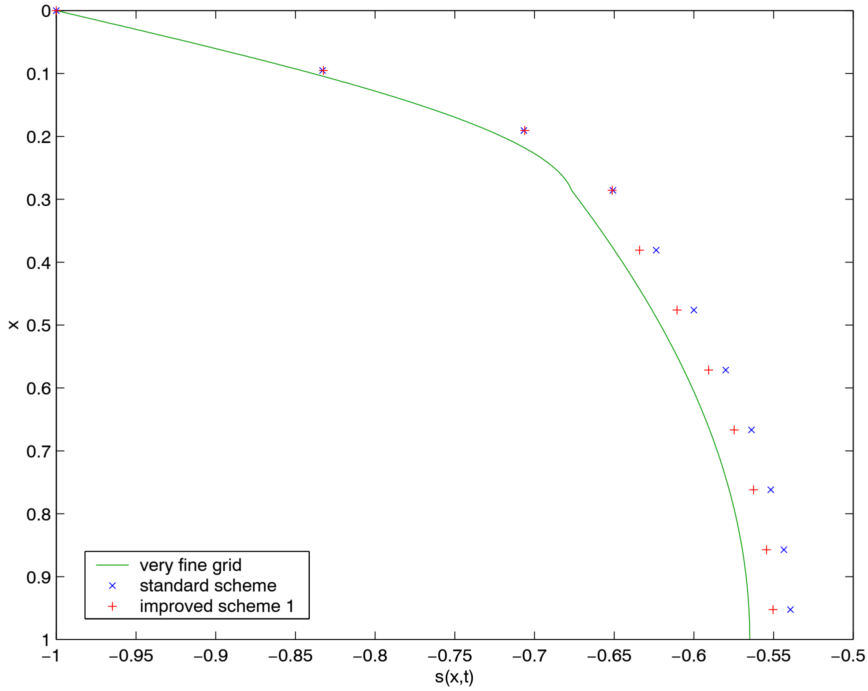

Figure 2: Example 1 - stress of the solid

5 Numerical experiments

Here we compare scheme (10) and modified scheme (57), (58), which gives better approximations for stresses. Detailed numerical experiments with (10) are presented in [4], where the order of convergence for all the variables is numerically studied, therefore here we illustrate only the calculation of stresses with the two schemes. Solid lines in the pictures below are solutions of the scheme (10), which are calculated on the very fine grids. Note that on such grids both schemes (basic and the modified one) give very similar results, which are not distinguishable on these pictures. The advantage of the modified scheme becomes evident on the coarse grids, and it is dependent on the input parameters,as it was discussed earlier (see inequalities (59) and (60)). Results from simulation of three examples are presented.

Example 1. Input data for the first experiment are as follows: $\zeta = \frac{2}{7}$, $\nu_1 = 1.0$, $\nu_2 = 50.0$, $k_1 = 1.0$, $k_2 = 0.5$. Comparison results at the time t=0.05 are depicted in the Fig. 2. We see that coarse grid solutions calculated with both schemes differ from the fine grid solution, however the modified scheme provides better approximation.

Example 2. In this experiment we choose following input parameters: $\zeta = \frac{2}{3}$, $\nu_1 = 1.0$, $\nu_2 = 0.01$, $k_1 = 1.0$, $k_2 = 0.1$, $t = 1.0$. As it can see from the Fig. 3, in this case the modified scheme gives very good approximation to fine grid solution even on coarse grid, and this is not the case for unmodified scheme.

Example 3. In the last example we demonstrate the situation when input parameters are such that performed modifications give almost no improvement because inequalities (59), (60) are valid. One can see it on the Fig. 4. Respective input parameters are: $\zeta = \frac{2}{3}$, $\nu_1 = 1.0$, $\nu_2 = 0.1$, $k_1 = 1.0$, $k_2 = 9.0$, $t = 0.1$.

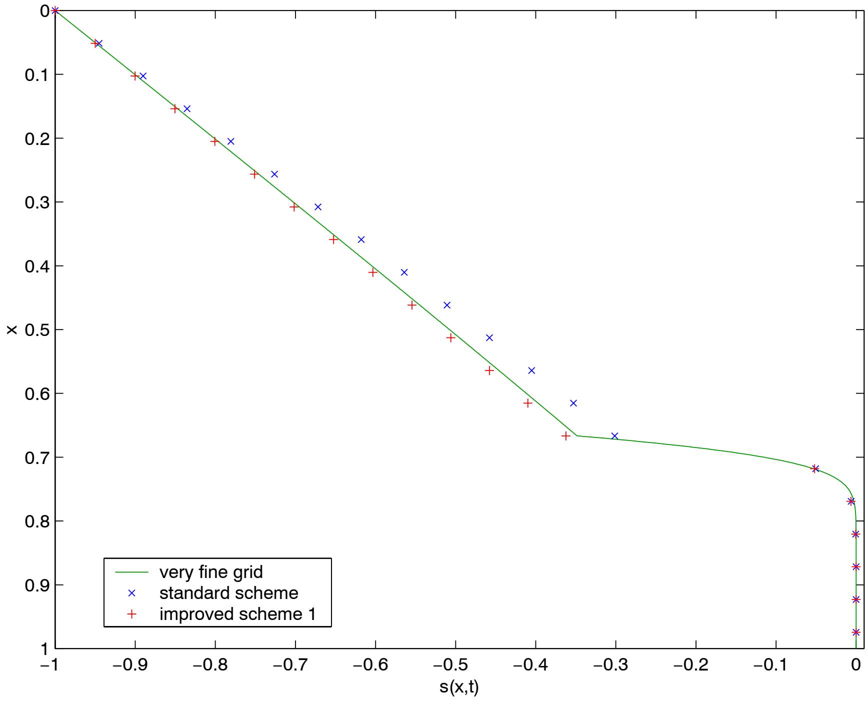

Figure 3: Example 2 - stress of the solid

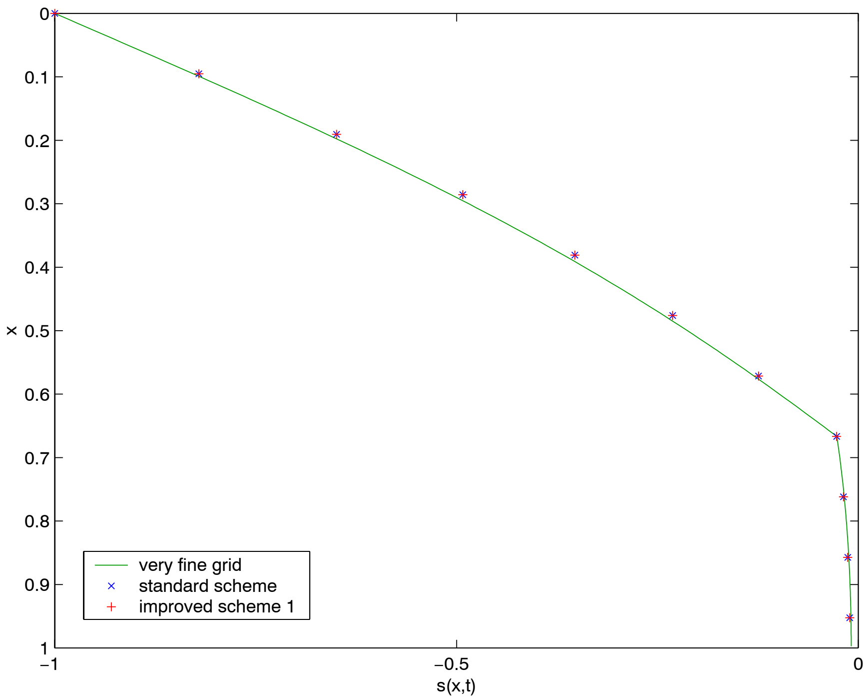

Figure 4: Example 3 - stress of the solid

References

[1] M. Biot, General theory of three dimensional consolidation, J. Appl. Phys., 12(1941), pp. 155-169.

[2] J. Bear, Y. Bachamat, Introduction to modelling of transport Phenomena in Porous Media, Kluwer Academic, Dordrecht, 1990.

[3] R.Ewing, O.Iliev, R.Lazarov, A modified finite volume approximation of second order elliptic equations with discontinuous coefficients, *SIAM J. Sci.Comp.*,vol.**23**,No.4, pp.1334-1350, 2001.

[4] F. Gaspar, O. Iliev, F. Lisbona, A. Naumovich, P. Vabishchevich: On numerical solution of 1-D poroelasticity equations in a multilayered domain Technical report Fraunhofer ITWM (66) 2004

[5] F.J. Gaspar, F.J. Lisbona, P.N. Vabischevich, A finite difference analysis of Biot's consolidation model, Appl. Num. Math, 44(2003), pp. 487-506.

[6] F.J. Gaspar, F.J. Lisbona, P.N. Vabischevich, A numerical model for radial flow through porous and deformable shells, CMAM, 4(2004), No.1 , pp. 34-47.

[7] R.W. Lewis, B.A. Schrefler, The finite element method in the static and dynamic deformation and consolidation of porous media, John Wiley, Chichester, 1998.

[8] A.Naumovich, O.Iliev, F.Gaspar, F.Lisbona, P.Vabishchevich, On numerical solution of 1-D poroelasticity equations in a multilayered domain, Technical report of Fraunhofer ITWM, 2004.

[9] A. A. Samarskii, Theory of difference schemes, Pure and Applied Mathematics, Marcel Dekker,New York, 2001.

[10] A. A. Smarskii, P. N. Vabischevich, P. P. Matus, Difference schemes with operator factors, Minsk, 1998.

[11] R.E. Showalter, Diffusion in poroelastic media, J. Math. Anal. Appl., 251 (2000), pp. 310-340.

[12] H. F. Wang, Theory of linear poroelasticity with application to geomechanics and hydrogeology, Princeton University Press, Princeton, 2000.

[13] L. Li, Theory of poroelastic structures with diffusion in the longitudinal directions, PhD thesis, Ben-Gurion University, Negev, US, 1997.

Published reports of the Fraunhofer ITWM

The PDF-files of the following reports are available under:
www.itwm.fraunhofer.de/de/zentral__berichte/berichte

1. D. Hietel, K. Steiner, J. Struckmeier

A Finite - Volume Particle Method for Compressible Flows

We derive a new class of particle methods for conservation laws, which are based on numerical flux functions to model the interactions between moving particles. The derivation is similar to that of classical Finite-Volume methods; except that the fixed grid structure in the Finite-Volume method is substituted by so-called mass packets of particles. We give some numerical results on a shock wave solution for Burgers equation as well as the well-known one-dimensional shock tube problem.
(19 pages, 1998)

2. M. Feldmann, S. Seibold

Damage Diagnosis of Rotors: Application of Hilbert Transform and Multi-Hypothesis Testing

In this paper, a combined approach to damage diagnosis of rotors is proposed. The intention is to employ signal-based as well as model-based procedures for an improved detection of size and location of the damage. In a first step, Hilbert transform signal processing techniques allow for a computation of the signal envelope and the instantaneous frequency, so that various types of non-linearities due to a damage may be identified and classified based on measured response data. In a second step, a multi-hypothesis bank of Kalman Filters is employed for the detection of the size and location of the damage based on the information of the type of damage provided by the results of the Hilbert transform.
Keywords: Hilbert transform, damage diagnosis, Kalman filtering, non-linear dynamics
(23 pages, 1998)

3. Y. Ben-Haim, S. Seibold

Robust Reliability of Diagnostic Multi-Hypothesis Algorithms: Application to Rotating Machinery

Damage diagnosis based on a bank of Kalman filters, each one conditioned on a specific hypothesized system condition, is a well recognized and powerful diagnostic tool. This multi-hypothesis approach can be applied to a wide range of damage conditions. In this paper, we will focus on the diagnosis of cracks in rotating machinery. The question we address is: how to optimize the multi-hypothesis algorithm with respect to the uncertainty of the spatial form and location of cracks and their resulting dynamic effects. First, we formulate a measure of the reliability of the diagnostic algorithm, and then we discuss modifications of the diagnostic algorithm for the maximization of the reliability. The reliability of a diagnostic algorithm is measured by the amount of uncertainty consistent with no-failure of the diagnosis. Uncertainty is quantitatively represented with convex models.
Keywords: Robust reliability, convex models, Kalman filtering, multi-hypothesis diagnosis, rotating machinery, crack diagnosis
(24 pages, 1998)

4. F.-Th. Lentes, N. Siedow

Three-dimensional Radiative Heat Transfer in Glass Cooling Processes

For the numerical simulation of 3D radiative heat transfer in glasses and glass melts, practically applicable mathematical methods are needed to handle such problems optimal using workstation class computers. Since the exact solution would require super-computer capabilities we concentrate on approximate solutions with a high degree of accuracy. The following approaches are studied: 3D diffusion approximations and 3D ray-tracing methods.
(23 pages, 1998)

5. A. Klar, R. Wegener

A hierarchy of models for multilane vehicular traffic
Part I: Modeling

In the present paper multilane models for vehicular traffic are considered. A microscopic multilane model based on reaction thresholds is developed. Based on this model an Enskog like kinetic model is developed. In particular, care is taken to incorporate the correlations between the vehicles. From the kinetic model a fluid dynamic model is derived. The macroscopic coefficients are deduced from the underlying kinetic model. Numerical simulations are presented for all three levels of description in [10]. Moreover, a comparison of the results is given there.
(23 pages, 1998)

Part II: Numerical and stochastic investigations

In this paper the work presented in [6] is continued. The present paper contains detailed numerical investigations of the models developed there. A numerical method to treat the kinetic equations obtained in [6] are presented and results of the simulations are shown. Moreover, the stochastic correlation model used in [6] is described and investigated in more detail.
(17 pages, 1998)

6. A. Klar, N. Siedow

Boundary Layers and Domain Decomposition for Radiative Heat Transfer and Diffusion Equations: Applications to Glass Manufacturing Processes

In this paper domain decomposition methods for radiative transfer problems including conductive heat transfer are treated. The paper focuses on semi-transparent materials, like glass, and the associated conditions at the interface between the materials. Using asymptotic analysis we derive conditions for the coupling of the radiative transfer equations and a diffusion approximation. Several test cases are treated and a problem appearing in glass manufacturing processes is computed. The results clearly show the advantages of a domain decomposition approach. Accuracy equivalent to the solution of the global radiative transfer solution is achieved, whereas computation time is strongly reduced.
(24 pages, 1998)

7. I. Choquet

Heterogeneous catalysis modelling and numerical simulation in rarified gas flows
Part I: Coverage locally at equilibrium

A new approach is proposed to model and simulate numerically heterogeneous catalysis in rarefied gas flows. It is developed to satisfy all together the following points:
1) describe the gas phase at the microscopic scale, as required in rarefied flows,
2) describe the wall at the macroscopic scale, to avoid prohibitive computational costs and consider not only crystalline but also amorphous surfaces,
3) reproduce on average macroscopic laws correlated with experimental results and
4) derive analytic models in a systematic and exact way. The problem is stated in the general framework of a non static flow in the vicinity of a catalytic and non porous surface (without aging). It is shown that the exact and systematic resolution method based on the Laplace transform, introduced previously by the author to model collisions in the gas phase, can be extended to the present problem. The proposed approach is applied to the modelling of the EleyRideal and LangmuirHinshelwood recombinations, assuming that the coverage is locally at equilibrium. The models are developed considering one atomic species and extended to the general case of several atomic species. Numerical calculations show that the models derived in this way reproduce with accuracy behaviors observed experimentally.
(24 pages, 1998)

8. J. Ohser, B. Steinbach, C. Lang

Efficient Texture Analysis of Binary Images

A new method of determining some characteristics of binary images is proposed based on a special linear filtering. This technique enables the estimation of the area fraction, the specific line length, and the specific integral of curvature. Furthermore, the specific length of the total projection is obtained, which gives detailed information about the texture of the image. The influence of lateral and directional resolution depending on the size of the applied filter mask is discussed in detail. The technique includes a method of increasing directional resolution for texture analysis while keeping lateral resolution as high as possible.
(17 pages, 1998)

9. J. Orlik

Homogenization for viscoelasticity of the integral type with aging and shrinkage

A multiphase composite with periodic distributed inclusions with a smooth boundary is considered in this contribution. The composite component materials are supposed to be linear viscoelastic and aging (of the nonconvolution integral type, for which the Laplace transform with respect to time is not effectively applicable) and are subjected to isotropic shrinkage. The free shrinkage deformation can be considered as a fictitious temperature deformation in the behavior law. The procedure presented in this paper proposes a way to determine average (effective homogenized) viscoelastic and shrinkage (temperature) composite properties and the homogenized stressfield from known properties of the components. This is done by the extension of the asymptotic homogenization technique known for pure elastic nonhomogeneous bodies to the nonhomogeneous thermoviscoelasticity of the integral nonconvolution type. Up to now, the homogenization theory has not covered viscoelasticity of the integral type. SanchezPalencia (1980), Francfort & Suquet (1987) (see [2], [9]) have considered homogenization for viscoelasticity of the differential form and only up to the first derivative order. The integralmodeled viscoelasticity is more general then the differential one and includes almost all known differential models. The homogenization procedure is based on the construction of an asymptotic solution with respect to a period of the composite structure. This reduces the original problem to some auxiliary boundary value problems of elasticity and viscoelasticity on the unit periodic cell, of the same type as the original non-homogeneous problem. The existence and uniqueness results for such problems were obtained for kernels satisfying some constrain conditions. This is done by the extension of the Volterra integral operator theory to the Volterra operators with respect to the time, whose 1 kernels are space linear operators for any fixed time variables. Some ideas of such approach were proposed in [11] and [12], where the Volterra operators with kernels depending additionally on parameter were considered. This manuscript delivers results of the same nature for the case of the spaceoperator kernels.
(20 pages, 1998)

10. J. Mohring

Helmholtz Resonators with Large Aperture

The lowest resonant frequency of a cavity resonator is usually approximated by the classical Helmholtz formula. However, if the opening is rather large and the front wall is narrow this formula is no longer valid. Here we present a correction which is of third order in the ratio of the diameters of aperture and cavity. In addition to the high accuracy it allows to estimate the damping due to radiation. The result is found by applying the method of matched asymptotic expansions. The correction contains form factors describing the shapes of opening and cavity. They are computed for a number of standard geometries. Results are compared with numerical computations.
(21 pages, 1998)

11. H. W. Hamacher, A. Schöbel

On Center Cycles in Grid Graphs

Finding "good" cycles in graphs is a problem of great interest in graph theory as well as in locational analysis. We show that the center and median problems are NP hard in general graphs. This result holds both for the variable cardinality case (i.e. all cycles of the graph are considered) and the fixed cardinality case (i.e. only cycles with a given cardinality p are feasible). Hence it is of interest to investigate special cases where the problem is solvable in polynomial time. In grid graphs, the variable cardinality case is, for instance, trivially solvable if the shape of the cycle can be chosen freely. If the shape is fixed to be a rectangle one can analyze rectangles in grid graphs with, in sequence, fixed dimension, fixed cardinality, and variable cardinality. In all cases a complete characterization of the optimal cycles and closed form expressions of the optimal objective values are given, yielding polynomial time algorithms for all cases of center rectangle problems. Finally, it is shown that center cycles can be chosen as rectangles for small cardinalities such that the center cycle problem in grid graphs is in these cases completely solved.
(15 pages, 1998)

12. H. W. Hamacher, K.-H. Küfer

Inverse radiation therapy planning - a multiple objective optimisation approach

For some decades radiation therapy has been proved successful in cancer treatment. It is the major task of clinical radiation treatment planning to realize on the one hand a high level dose of radiation in the cancer tissue in order to obtain maximum tumor control. On the other hand it is obvious that it is absolutely necessary to keep in the tissue outside the tumor, particularly in organs at risk, the unavoidable radiation as low as possible.
No doubt, these two objectives of treatment planning - high level dose in the tumor, low radiation outside the tumor - have a basically contradictory nature. Therefore, it is no surprise that inverse mathematical models with dose distribution bounds tend to be infeasible in most cases. Thus, there is need for approximations compromising between overdosing the organs at risk and underdosing the target volume.
Differing from the currently used time consuming iterative approach, which measures deviation from an ideal (non-achievable) treatment plan using recursively trial-and-error weights for the organs of interest, we go a new way trying to avoid a priori weight choices and consider the treatment planning problem as a multiple objective linear programming problem: with each organ of interest, target tissue as well as organs at risk, we associate an objective function measuring the maximal deviation from the prescribed doses.
We build up a data base of relatively few efficient solutions representing and approximating the variety of Pareto solutions of the multiple objective linear programming problem. This data base can be easily scanned by physicians looking for an adequate treatment plan with the aid of an appropriate online tool.
(14 pages, 1999)

13. C. Lang, J. Ohser, R. Hilfer

On the Analysis of Spatial Binary Images

This paper deals with the characterization of microscopically heterogeneous, but macroscopically homogeneous spatial structures. A new method is presented which is strictly based on integral-geometric formulae such as Crofton's intersection formulae and Hadwiger's recursive definition of the Euler number. The corresponding algorithms have clear advantages over other techniques. As an example of application we consider the analysis of spatial digital images produced by means of Computer Assisted Tomography.
(20 pages, 1999)

14. M. Junk

On the Construction of Discrete Equilibrium Distributions for Kinetic Schemes

A general approach to the construction of discrete equilibrium distributions is presented. Such distribution functions can be used to set up Kinetic Schemes as well as Lattice Boltzmann methods. The general principles are also applied to the construction of Chapman Enskog distributions which are used in Kinetic Schemes for compressible Navier-Stokes equations.
(24 pages, 1999)

15. M. Junk, S. V. Raghurame Rao

A new discrete velocity method for Navier-Stokes equations

The relation between the Lattice Boltzmann Method, which has recently become popular, and the Kinetic Schemes, which are routinely used in Computational Fluid Dynamics, is explored. A new discrete velocity model for the numerical solution of Navier-Stokes equations for incompressible fluid flow is presented by combining both the approaches. The new scheme can be interpreted as a pseudo-compressibility method and, for a particular choice of parameters, this interpretation carries over to the Lattice Boltzmann Method.
(20 pages, 1999)

16. H. Neunzert

Mathematics as a Key to Key Technologies

The main part of this paper will consist of examples, how mathematics really helps to solve industrial problems; these examples are taken from our Institute for Industrial Mathematics, from research in the Technomathematics group at my university, but also from ECMI groups and a company called TecMath, which originated 10 years ago from my university group and has already a very successful history.
(39 pages (4 PDF-Files), 1999)

17. J. Ohser, K. Sandau

Considerations about the Estimation of the Size Distribution in Wicksell's Corpuscle Problem

Wicksell's corpuscle problem deals with the estimation of the size distribution of a population of particles, all having the same shape, using a lower dimensional sampling probe. This problem was originary formulated for particle systems occurring in life sciences but its solution is of actual and increasing interest in materials science. From a mathematical point of view, Wicksell's problem is an inverse problem where the interesting size distribution is the unknown part of a Volterra equation. The problem is often regarded ill-posed, because the structure of the integrand implies unstable numerical solutions. The accuracy of the numerical solutions is considered here using the condition number, which allows to compare different numerical methods with different (equidistant) class sizes and which indicates, as one result, that a finite section thickness of the probe reduces the numerical problems. Furthermore, the relative error of estimation is computed which can be split into two parts. One part consists of the relative discretization error that increases for increasing class size, and the second part is related to the relative statistical error which increases with decreasing class size. For both parts, upper bounds can be given and the sum of them indicates an optimal class width depending on some specific constants.
(18 pages, 1999)

18. E. Carrizosa, H. W. Hamacher, R. Klein, S. Nickel

Solving nonconvex planar location problems by finite dominating sets

It is well-known that some of the classical location problems with polyhedral gauges can be solved in polynomial time by finding a finite dominating set, i. e. a finite set of candidates guaranteed to contain at least one optimal location.
In this paper it is first established that this result holds for a much larger class of problems than currently considered in the literature. The model for which this result can be proven includes, for instance, location problems with attraction and repulsion, and location-allocation problems.
Next, it is shown that the approximation of general gauges by polyhedral ones in the objective function of our general model can be analyzed with regard to the subsequent error in the optimal objective value. For the approximation problem two different approaches are described, the sandwich procedure and the greedy algorithm. Both of these approaches lead - for fixed epsilon - to polynomial approximation algorithms with accuracy epsilon for solving the general model considered in this paper.
Keywords: Continuous Location, Polyhedral Gauges, Finite Dominating Sets, Approximation, Sandwich Algorithm, Greedy Algorithm
(19 pages, 2000)

19. A. Becker

A Review on Image Distortion Measures

Within this paper we review image distortion measures. A distortion measure is a criterion that assigns a "quality number" to an image. We distinguish between mathematical distortion measures and those distortion measures in-cooperating a priori knowledge about the imaging devices (e. g. satellite images), image processing algorithms or the human physiology. We will consider representative examples of different kinds of distortion measures and are going to discuss them.
Keywords: Distortion measure, human visual system
(26 pages, 2000)

20. H. W. Hamacher, M. Labbé, S. Nickel, T. Sonneborn

Polyhedral Properties of the Uncapacitated Multiple Allocation Hub Location Problem

We examine the feasibility polyhedron of the uncapacitated hub location problem (UHL) with multiple allocation, which has applications in the fields of air passenger and cargo transportation, telecommunication and postal delivery services. In particular we determine the dimension and derive some classes of facets of this polyhedron. We develop some general rules about lifting facets from the uncapacitated facility location (UFL) for UHL and projecting facets from UHL to UFL. By applying these rules we get a new class of facets for UHL which dominates the inequalities in the original formulation. Thus we get a new formulation of UHL whose constraints are all facet–defining. We show its superior computational performance by benchmarking it on a well known data set.
Keywords: integer programming, hub location, facility location, valid inequalities, facets, branch and cut
(21 pages, 2000)

21. H. W. Hamacher, A. Schöbel

Design of Zone Tariff Systems in Public Transportation

Given a public transportation system represented by its stops and direct connections between stops, we consider two problems dealing with the prices for the customers: The fare problem in which subsets of stops are already aggregated to zones and "good" tariffs have to be found in the existing zone system. Closed form solutions for the fare problem are presented for three objective functions. In the zone problem the design of the zones is part of the problem. This problem is NP hard and we therefore propose three heuristics which prove to be very successful in the redesign of one of Germany's transportation systems.
(30 pages, 2001)

22. D. Hietel, M. Junk, R. Keck, D. Teleaga

The Finite-Volume-Particle Method for Conservation Laws

In the Finite-Volume-Particle Method (FVPM), the weak formulation of a hyperbolic conservation law is discretized by restricting it to a discrete set of test functions. In contrast to the usual Finite-Volume approach, the test functions are not taken as characteristic functions of the control volumes in a spatial grid, but are chosen from a partition of unity with smooth and overlapping partition functions (the particles), which can even move along pre- scribed velocity fields. The information exchange between particles is based on standard numerical flux functions. Geometrical information, similar to the surface area of the cell faces in the Finite-Volume Method and the corresponding normal directions are given as integral quantities of the partition functions. After a brief derivation of the Finite-Volume-Particle Method, this work focuses on the role of the geometric coefficients in the scheme.
(16 pages, 2001)

23. T. Bender, H. Hennes, J. Kalcsics, M. T. Melo, S. Nickel

Location Software and Interface with GIS and Supply Chain Management

The objective of this paper is to bridge the gap between location theory and practice. To meet this objective focus is given to the development of software capable of addressing the different needs of a wide group of users. There is a very active community on location theory encompassing many research fields such as operations research, computer science, mathematics, engineering, geography, economics and marketing. As a result, people working on facility location problems have a very diverse background and also different needs regarding the software to solve these problems. For those interested in non-commercial applications (e. g. students and researchers), the library of location algorithms (LoLA can be of considerable assistance. LoLA contains a collection of efficient algorithms for solving planar, network and discrete facility location problems. In this paper, a detailed description of the functionality of LoLA is presented. In the fields of geography and marketing, for instance, solving facility location problems requires using large amounts of demographic data. Hence, members of these groups (e. g. urban planners and sales managers) often work with geographical information too s. To address the specific needs of these users, LoLA was inked to a geographical information system (GIS) and the details of the combined functionality are described in the paper. Finally, there is a wide group of practitioners who need to solve large problems and require special purpose software with a good data interface. Many of such users can be found, for example, in the area of supply chain management (SCM). Logistics activities involved in strategic SCM include, among others, facility location planning. In this paper, the development of a commercial location software tool is also described. The too is embedded in the Advanced Planner and Optimizer SCM software developed by SAP AG, Walldorf, Germany. The paper ends with some conclusions and an outlook to future activities.
Keywords: facility location, software development, geographical information systems, supply chain management
(48 pages, 2001)

24. H. W. Hamacher, S. A. Tjandra

Mathematical Modelling of Evacuation Problems: A State of Art

This paper details models and algorithms which can be applied to evacuation problems. While it concentrates on building evacuation many of the results are applicable also to regional evacuation. All models consider the time as main parameter, where the travel time between components of the building is part of the input and the overall evacuation time is the output. The paper distinguishes between macroscopic and microscopic evacuation models both of which are able to capture the evacuees' movement over time.
Macroscopic models are mainly used to produce good lower bounds for the evacuation time and do not consider any individual behavior during the emergency situation. These bounds can be used to analyze existing buildings or help in the design phase of planning a building. Macroscopic approaches which are based on dynamic network flow models (minimum cost dynamic flow, maximum dynamic flow, universal maximum flow, quickest path and quickest flow) are described. A special feature of the presented approach is the fact, that travel times of evacuees are not restricted to be constant, but may be density dependent. Using multicriteria optimization priority regions and blockage due to fire or smoke may be considered. It is shown how the modelling can be done using time parameter either as discrete or continuous parameter.
Microscopic models are able to model the individual evacuee's characteristics and the interaction among evacuees which influence their movement. Due to the corresponding huge amount of data one uses simulation approaches. Some probabilistic laws for individual evacuee's movement are presented. Moreover ideas to model the evacuee's movement using cellular automata (CA) and resulting software are presented.
In this paper we will focus on macroscopic models and only summarize some of the results of the microscopic approach. While most of the results are applicable to general evacuation situations, we concentrate on building evacuation.
(44 pages, 2001)

25. J. Kuhnert, S. Tiwari

Grid free method for solving the Poisson equation

A Grid free method for solving the Poisson equation is presented. This is an iterative method. The method is based on the weighted least squares approximation in which the Poisson equation is enforced to be satisfied in every iterations. The boundary conditions can also be enforced in the iteration process. This is a local approximation procedure. The Dirichlet, Neumann and mixed boundary value problems on a unit square are presented and the analytical solutions are compared with the exact solutions. Both solutions matched perfectly.
Keywords: Poisson equation, Least squares method, Grid free method
(19 pages, 2001)

26. T. Götz, H. Rave, D. Reinel-Bitzer, K. Steiner, H. Tiemeier

Simulation of the fiber spinning process

To simulate the influence of process parameters to the melt spinning process a fiber model is used and coupled with CFD calculations of the quench air flow. In the fiber model energy, momentum and mass balance are solved for the polymer mass flow. To calculate the quench air the Lattice Boltzmann method is used. Simulations and experiments for different process parameters and hole configurations are compared and show a good agreement.
Keywords: Melt spinning, fiber model, Lattice Boltzmann, CFD
(19 pages, 2001)

27. A. Zemitis

On interaction of a liquid film with an obstacle

In this paper mathematical models for liquid films generated by impinging jets are discussed. Attention is stressed to the interaction of the liquid film with some obstacle. S. G. Taylor [Proc. R. Soc. London Ser. A 253, 313 (1959)] found that the liquid film generated by impinging jets is very sensitive to properties of the wire which was used as an obstacle. The aim of this presentation is to propose a modification of the Taylor's model, which allows to simulate the film shape in cases, when the angle between jets is different from 180°. Numerical results obtained by discussed models give two different shapes of the liquid film similar as in Taylors experiments. These two shapes depend on the regime: either droplets are produced close to the obstacle or not. The difference between two regimes becomes larger if the angle between jets decreases. Existence of such two regimes can be very essential for some applications of impinging jets, if the generated liquid film can have a contact with obstacles.
Keywords: impinging jets, liquid film, models, numerical solution, shape
(22 pages, 2001)

28. I. Ginzburg, K. Steiner

Free surface lattice-Boltzmann method to model the filling of expanding cavities by Bingham Fluids

The filling process of viscoplastic metal alloys and plastics in expanding cavities is modelled using the lattice Boltzmann method in two and three dimensions. These models combine the regularized Bingham model for viscoplastic with a free-interface algorithm. The latter is based on a modified immiscible lattice Boltzmann model in which one species is the fluid and the other one is considered as vacuum. The boundary conditions at the curved liquid-vacuum interface are met without any geometrical front reconstruction from a first-order Chapman-Enskog expansion. The numerical results obtained with these models are found in good agreement with available theoretical and numerical analysis.
Keywords: Generalized LBE, free-surface phenomena, interface boundary conditions, filling processes, Bingham viscoplastic model, regularized models
(22 pages, 2001)

29. H. Neunzert

»Denn nichts ist für den Menschen als Menschen etwas wert, was er nicht mit Leidenschaft tun kann«
Vortrag anlässlich der Verleihung des Akademiepreises des Landes Rheinland-Pfalz am 21.11.2001

Was macht einen guten Hochschullehrer aus? Auf diese Frage gibt es sicher viele verschiedene, fachbezogene Antworten, aber auch ein paar allgemeine Gesichtspunkte: es bedarf der »Leidenschaft« für die Forschung (Max Weber), aus der dann auch die Begeisterung für die Lehre erwächst. Forschung und Lehre gehören zusammen, um die Wissenschaft als lebendiges Tun vermitteln zu können. Der Vortrag gibt Beispiele dafür, wie in angewandter Mathematik Forschungsaufgaben aus praktischen Alltagsproblemstellungen erwachsen, die in die Lehre auf verschiedenen Stufen (Gymnasium bis Graduiertenkolleg) einfließen; er leitet damit auch zu einem aktuellen Forschungsgebiet, der Mehrskalenanalyse mit ihren vielfältigen Anwendungen in Bildverarbeitung, Materialentwicklung und Strömungsmechanik über, was aber nur kurz gestreift wird. Mathematik erscheint hier als eine moderne Schlüsseltechnologie, die aber auch enge Beziehungen zu den Geistes- und Sozialwissenschaften hat.
Keywords: Lehre, Forschung, angewandte Mathematik, Mehrskalenanalyse, Strömungsmechanik
(18 pages, 2001)

30. J. Kuhnert, S. Tiwari

Finite pointset method based on the projection method for simulations of the incompressible Navier-Stokes equations

A Lagrangian particle scheme is applied to the projection method for the incompressible Navier-Stokes equations. The approximation of spatial derivatives is obtained by the weighted least squares method. The pressure Poisson equation is solved by a local iterative procedure with the help of the least squares method. Numerical tests are performed for two dimensional cases. The Couette flow, Poiseuelle flow, decaying shear flow and the driven cavity flow are presented. The numerical solutions are obtained for stationary as well as instationary cases and are compared with the analytical solutions for channel flows. Finally, the driven cavity in a unit square is considered and the stationary solution obtained from this scheme is compared with that from the finite element method.
Keywords: Incompressible Navier-Stokes equations, Meshfree method, Projection method, Particle scheme, Least squares approximation
AMS subject classification: 76D05, 76M28
(25 pages, 2001)

31. R. Korn, M. Krekel

Optimal Portfolios with Fixed Consumption or Income Streams

We consider some portfolio optimisation problems where either the investor has a desire for an a priori specified consumption stream or/and follows a deterministic pay in scheme while also trying to maximize expected utility from final wealth. We derive explicit closed form solutions for continuous and discrete monetary streams. The mathematical method used is classical stochastic control theory.
Keywords: Portfolio optimisation, stochastic control, HJB equation, discretisation of control problems.
(23 pages, 2002)

32. M. Krekel

Optimal portfolios with a loan dependent credit spread

If an investor borrows money he generally has to pay higher interest rates than he would have received, if he had put his funds on a savings account. The classical model of continuous time portfolio optimisation ignores this effect. Since there is obviously a connection between the default probability and the total

percentage of wealth, which the investor is in debt, we study portfolio optimisation with a control dependent interest rate. Assuming a logarithmic and a power utility function, respectively, we prove explicit formulae of the optimal control.
Keywords: Portfolio optimisation, stochastic control, HJB equation, credit spread, log utility, power utility, non-linear wealth dynamics
(25 pages, 2002)

33. J. Ohser, W. Nagel, K. Schladitz

The Euler number of discretized sets - on the choice of adjacency in homogeneous lattices

Two approaches for determining the Euler-Poincaré characteristic of a set observed on lattice points are considered in the context of image analysis { the integral geometric and the polyhedral approach. Information about the set is assumed to be available on lattice points only. In order to retain properties of the Euler number and to provide a good approximation of the true Euler number of the original set in the Euclidean space, the appropriate choice of adjacency in the lattice for the set and its background is crucial. Adjacencies are defined using tessellations of the whole space into polyhedrons. In R 3 , two new 14 adjacencies are introduced additionally to the well known 6 and 26 adjacencies. For the Euler number of a set and its complement, a consistency relation holds. Each of the pairs of adjacencies (14:1; 14:1), (14:2; 14:2), (6; 26), and (26; 6) is shown to be a pair of complementary adjacencies with respect to this relation. That is, the approximations of the Euler numbers are consistent if the set and its background (complement) are equipped with this pair of adjacencies. Furthermore, sufficient conditions for the correctness of the approximations of the Euler number are given. The analysis of selected microstructures and a simulation study illustrate how the estimated Euler number depends on the chosen adjacency. It also shows that there is not a uniquely best pair of adjacencies with respect to the estimation of the Euler number of a set in Euclidean space.
Keywords: image analysis, Euler number, neighborhod relationships, cuboidal lattice
(32 pages, 2002)

34. I. Ginzburg, K. Steiner

Lattice Boltzmann Model for Free-Surface flow and Its Application to Filling Process in Casting

A generalized lattice Boltzmann model to simulate free-surface is constructed in both two and three dimensions. The proposed model satisfies the interfacial boundary conditions accurately. A distinctive feature of the model is that the collision processes is carried out only on the points occupied partially or fully by the fluid. To maintain a sharp interfacial front, the method includes an anti-diffusion algorithm. The unknown distribution functions at the interfacial region are constructed according to the first order Chapman-Enskog analysis. The interfacial boundary conditions are satisfied exactly by the coefficients in the Chapman-Enskog expansion. The distribution functions are naturally expressed in the local interfacial coordinates. The macroscopic quantities at the interface are extracted from the least-square solutions of a locally linearized system obtained from the known distribution functions. The proposed method does not require any geometric front construction and is robust for any interfacial topology. Simulation results of realistic filling process are presented: rectangular cavity in two dimensions and Hammer box, Campbell box, Sheffield box, and Motorblock in three dimensions. To enhance the stability at high Reynolds numbers, various upwind-type schemes are developed. Free-slip and no-slip boundary conditions are also discussed.
Keywords: Lattice Boltzmann models; free-surface phenomena; interface boundary conditions; filling processes; injection molding; volume of fluid method; interface boundary conditions; advection-schemes; upwind-schemes
(54 pages, 2002)

35. M. Günther, A. Klar, T. Materne, R. Wegener

Multivalued fundamental diagrams and stop and go waves for continuum traffic equations

In the present paper a kinetic model for vehicular traffic leading to multivalued fundamental diagrams is developed and investigated in detail. For this model phase transitions can appear depending on the local density and velocity of the flow. A derivation of associated macroscopic traffic equations from the kinetic equation is given. Moreover, numerical experiments show the appearance of stop and go waves for highway traffic with a bottleneck.
Keywords: traffic flow, macroscopic equations, kinetic derivation, multivalued fundamental diagram, stop and go waves, phase transitions
(25 pages, 2002)

36. S. Feldmann, P. Lang, D. Prätzel-Wolters

Parameter influence on the zeros of network determinants

To a network N(q) with determinant D(s;q) depending on a parameter vector q Î Rr via identification of some of its vertices, a network N^ (q) is assigned. The paper deals with procedures to find N^ (q), such that its determinant D^ (s;q) admits a factorization in the determinants of appropriate subnetworks, and with the estimation of the deviation of the zeros of D^ from the zeros of D. To solve the estimation problem state space methods are applied.
Keywords: Networks, Equicofactor matrix polynomials, Realization theory, Matrix perturbation theory
(30 pages, 2002)

37. K. Koch, J. Ohser, K. Schladitz

Spectral theory for random closed sets and estimating the covariance via frequency space

A spectral theory for stationary random closed sets is developed and provided with a sound mathematical basis. Definition and proof of existence of the Bartlett spectrum of a stationary random closed set as well as the proof of a Wiener-Khintchine theorem for the power spectrum are used to two ends: First, well known second order characteristics like the covariance can be estimated faster than usual via frequency space. Second, the Bartlett spectrum and the power spectrum can be used as second order characteristics in frequency space. Examples show, that in some cases information about the random closed set is easier to obtain from these characteristics in frequency space than from their real world counterparts.
Keywords: Random set, Bartlett spectrum, fast Fourier transform, power spectrum
(28 pages, 2002)

38. D. d'Humières, I. Ginzburg

Multi-reflection boundary conditions for lattice Boltzmann models

We present a unified approach of several boundary conditions for lattice Boltzmann models. Its general framework is a generalization of previously introduced schemes such as the bounce-back rule, linear or quadratic interpolations, etc. The objectives are two fold: first to give theoretical tools to study the existing boundary conditions and their corresponding accuracy; secondly to design formally third- order accurate boundary conditions for general flows. Using these boundary conditions, Couette and Poiseuille flows are exact solution of the lattice Boltzmann models for a Reynolds number Re = 0 (Stokes limit).
Numerical comparisons are given for Stokes flows in periodic arrays of spheres and cylinders, linear periodic array of cylinders between moving plates and for Navier-Stokes flows in periodic arrays of cylinders for Re < 200. These results show a significant improvement of the overall accuracy when using the linear interpolations instead of the bounce-back reflection (up to an order of magnitude on the hydrodynamics fields). Further improvement is achieved with the new multi-reflection boundary conditions, reaching a level of accuracy close to the quasi-analytical reference solutions, even for rather modest grid resolutions and few points in the narrowest channels. More important, the pressure and velocity fields in the vicinity of the obstacles are much smoother with multi-reflection than with the other boundary conditions.
Finally the good stability of these schemes is highlighted by some simulations of moving obstacles: a cylinder between flat walls and a sphere in a cylinder.
Keywords: lattice Boltzmann equation, boudary condistions, bounce-back rule, Navier-Stokes equation
(72 pages, 2002)

39. R. Korn

Elementare Finanzmathematik

Im Rahmen dieser Arbeit soll eine elementar gehaltene Einführung in die Aufgabenstellungen und Prinzipien der modernen Finanzmathematik gegeben werden. Insbesondere werden die Grundlagen der Modellierung von Aktienkursen, der Bewertung von Optionen und der Portfolio-Optimierung vorgestellt. Natürlich können die verwendeten Methoden und die entwickelte Theorie nicht in voller Allgemeinheit für den Schulunterricht verwendet werden, doch sollen einzelne Prinzipien so heraus gearbeitet werden, dass sie auch an einfachen Beispielen verstanden werden können.
Keywords: Finanzmathematik, Aktien, Optionen, Portfolio-Optimierung, Börse, Lehrerweiterbildung, Mathematikunterricht
(98 pages, 2002)

40. J. Kallrath, M. C. Müller, S. Nickel

Batch Presorting Problems: Models and Complexity Results

In this paper we consider short term storage systems. We analyze presorting strategies to improve the effiency of these storage systems. The presorting task is called Batch PreSorting Problem (BPSP). The BPSP is a variation of an assigment problem, i. e., it has an assigment problem kernel and some additional constraints. We present different types of these presorting problems, introduce mathematical programming formulations and prove the NP-completeness for one type of the BPSP. Experiments are carried out in order to compare the different model formulations and to investigate the behavior of these models.
Keywords: Complexity theory, Integer programming, Assigment, Logistics
(19 pages, 2002)

41. J. Linn

On the frame-invariant description of the phase space of the Folgar-Tucker equation

The Folgar-Tucker equation is used in flow simulations of fiber suspensions to predict fiber orientation depending on the local flow. In this paper, a complete, frame-invariant description of the phase space of this differential equation is presented for the first time.
Key words: fiber orientation, Folgar-Tucker equation, injection molding
(5 pages, 2003)

42. T. Hanne, S. Nickel

A Multi-Objective Evolutionary Algorithm for Scheduling and Inspection Planning in Software Development Projects

In this article, we consider the problem of planning inspections and other tasks within a software development (SD) project with respect to the objectives quality (no. of defects), project duration, and costs. Based on a discrete-event simulation model of SD processes comprising the phases coding, inspection, test, and rework, we present a simplified formulation of the problem as a multiobjective optimization problem. For solving the problem (i. e. finding an approximation of the efficient set) we develop a multiobjective evolutionary algorithm. Details of the algorithm are discussed as well as results of its application to sample problems.
Key words: multiple objective programming, project management and scheduling, software development, evolutionary algorithms, efficient set
(29 pages, 2003)

43. T. Bortfeld , K.-H. Küfer, M. Monz, A. Scherrer, C. Thieke, H. Trinkaus

Intensity-Modulated Radiotherapy - A Large Scale Multi-Criteria Programming Problem -

Radiation therapy planning is always a tight rope walk between dangerous insufficient dose in the target volume and life threatening overdosing of organs at risk. Finding ideal balances between these inherently contradictory goals challenges dosimetrists and physicians in their daily practice. Today's planning systems are typically based on a single evaluation function that measures the quality of a radiation treatment plan. Unfortunately, such a one dimensional approach cannot satisfactorily map the different backgrounds of physicians and the patient dependent necessities. So, too often a time consuming iteration process between evaluation of dose distribution and redefinition of the evaluation function is needed.
In this paper we propose a generic multi-criteria approach based on Pareto's solution concept. For each entity of interest - target volume or organ at risk a structure dependent evaluation function is defined measuring deviations from ideal doses that are calculated from statistical functions. A reasonable bunch of clinically meaningful Pareto optimal solutions are stored in a data base, which can be interactively searched by physicians. The system guarantees dynamical planning as well as the discussion of tradeoffs between different entities.
Mathematically, we model the upcoming inverse problem as a multi-criteria linear programming problem. Because of the large scale nature of the problem it is not possible to solve the problem in a 3D-setting without adaptive reduction by appropriate approximation schemes.
Our approach is twofold: First, the discretization of the continuous problem is based on an adaptive hierarchical clustering process which is used for a local refinement of constraints during the optimization procedure. Second, the set of Pareto optimal solutions is approximated by an adaptive grid of representatives that are found by a hybrid process of calculating extreme compromises and interpolation methods.
Keywords: multiple criteria optimization, representative systems of Pareto solutions, adaptive triangulation, clustering and disaggregation techniques, visualization of Pareto solutions, medical physics, external beam radiotherapy planning, intensity modulated radiotherapy
(31 pages, 2003)

44. T. Halfmann, T. Wichmann

Overview of Symbolic Methods in Industrial Analog Circuit Design

Industrial analog circuits are usually designed using numerical simulation tools. To obtain a deeper circuit understanding, symbolic analysis techniques can additionally be applied. Approximation methods which reduce the complexity of symbolic expressions are needed in order to handle industrial-sized problems.
This paper will give an overview to the field of symbolic analog circuit analysis. Starting with a motivation, the state-of-the-art simplification algorithms for linear as well as for nonlinear circuits are presented. The basic ideas behind the different techniques are described, whereas the technical details can be found in the cited references. Finally, the application of linear and nonlinear symbolic analysis will be shown on two example circuits.
Keywords: CAD, automated analog circuit design, symbolic analysis, computer algebra, behavioral modeling, system simulation, circuit sizing, macro modeling, differential-algebraic equations, index
(17 pages, 2003)

45. S. E. Mikhailov, J. Orlik

Asymptotic Homogenisation in Strength and Fatigue Durability Analysis of Composites

Asymptotic homogenisation technique and two-scale convergence is used for analysis of macro-strength and fatigue durability of composites with a periodic structure under cyclic loading. The linear damage accumulation rule is employed in the phenomenological micro-durability conditions (for each component of the composite) under varying cyclic loading. Both local and non-local strength and durability conditions are analysed. The strong convergence of the strength and fatigue damage measure as the structure period tends to zero is proved and their limiting values are estimated.
Keywords: multiscale structures, asymptotic homogenization, strength, fatigue, singularity, non-local conditions
(14 pages, 2003)

46. P. Domínguez-Marín, P. Hansen, N. Mladenović , S. Nickel

Heuristic Procedures for Solving the Discrete Ordered Median Problem

We present two heuristic methods for solving the Discrete Ordered Median Problem (DOMP), for which no such approaches have been developed so far. The DOMP generalizes classical discrete facility location problems, such as the p-median, p-center and Uncapacitated Facility Location problems. The first procedure proposed in this paper is based on a genetic algorithm developed by Moreno Vega [MV96] for p-median and p-center problems. Additionally, a second heuristic approach based on the Variable Neighborhood Search metaheuristic (VNS) proposed by Hansen & Mladenovic [HM97] for the p-median problem is described. An extensive numerical study is presented to show the efficiency of both heuristics and compare them.
Keywords: genetic algorithms, variable neighborhood search, discrete facility location
(31 pages, 2003)

47. N. Boland, P. Domínguez-Marín, S. Nickel, J. Puerto

Exact Procedures for Solving the Discrete Ordered Median Problem

The Discrete Ordered Median Problem (DOMP) generalizes classical discrete location problems, such as the N-median, N-center and Uncapacitated Facility Location problems. It was introduced by Nickel [16], who formulated it as both a nonlinear and a linear integer program. We propose an alternative integer linear programming formulation for the DOMP, discuss relationships between both integer linear programming formulations, and show how properties of optimal solutions can be used to strengthen these formulations. Moreover, we present a specific branch and bound procedure to solve the DOMP more efficiently. We test the integer linear programming formulations and this branch and bound method computationally on randomly generated test problems.
Keywords: discrete location, Integer programming
(41 pages, 2003)

48. S. Feldmann, P. Lang

Padé-like reduction of stable discrete linear systems preserving their stability

A new stability preserving model reduction algorithm for discrete linear SISO-systems based on their impulse response is proposed. Similar to the Padé approximation, an equation system for the Markov parameters involving the Hankel matrix is considered, that here however is chosen to be of very high dimension. Although this equation system therefore in general cannot be solved exactly, it is proved that the approximate solution, computed via the Moore-Penrose inverse, gives rise to a stability preserving reduction scheme, a property that cannot be guaranteed for the Padé approach. Furthermore, the proposed algorithm is compared to another stability preserving reduction approach, namely the balanced truncation method, showing comparable performance of the reduced systems. The balanced truncation method however starts from a state space description of the systems and in general is expected to be more computational demanding.
Keywords: Discrete linear systems, model reduction, stability, Hankel matrix, Stein equation
(16 pages, 2003)

49. J. Kallrath, S. Nickel

A Polynomial Case of the Batch Presorting Problem

This paper presents new theoretical results for a special case of the batch presorting problem (BPSP). We will show tht this case can be solved in polynomial time. Offline and online algorithms are presented for solving the BPSP. Competetive analysis is used for comparing the algorithms.
Keywords: batch presorting problem, online optimization, competetive analysis, polynomial algorithms, logistics
(17 pages, 2003)

50. T. Hanne, H. L. Trinkaus

knowCube for MCDM – Visual and Interactive Support for Multicriteria Decision Making

In this paper, we present a novel multicriteria decision support system (MCDSS), called knowCube, consisting of components for knowledge organization, generation, and navigation. Knowledge organization rests upon a database for managing qualitative and quantitative criteria, together with add-on information. Knowledge generation serves filling the database via e. g. identification, optimization, classification or simulation. For "finding needles in haycocks", the knowledge navigation component supports graphical database retrieval and interactive, goal-oriented problem solving. Navigation "helpers" are, for instance, cascading criteria aggregations, modifiable metrics, ergonomic interfaces, and customizable visualizations. Examples from real-life projects, e.g. in industrial engineering and in the life sciences, illustrate the application of our MCDSS.
Key words: Multicriteria decision making, knowledge management, decision support systems, visual interfaces, interactive navigation, real-life applications.
(26 pages, 2003)

51. O. Iliev, V. Laptev

On Numerical Simulation of Flow Through Oil Filters

This paper concerns numerical simulation of flow through oil filters. Oil filters consist of filter housing (filter box), and a porous filtering medium, which completely separates the inlet from the outlet. We discuss mathematical models, describing coupled flows in the pure liquid subregions and in the porous filter media, as well as interface conditions between them. Further, we reformulate the problem in fictitious regions method manner, and discuss peculiarities of the numerical algorithm in solving the coupled system. Next, we show numerical results, validating the model and the algorithm. Finally, we present results from simulation of 3-D oil flow through a real car filter.
Keywords: oil filters, coupled flow in plain and porous media, Navier-Stokes, Brinkman, numerical simulation
(8 pages, 2003)

52. W. Dörfler, O. Iliev, D. Stoyanov, D. Vassileva

On a Multigrid Adaptive Refinement Solver for Saturated Non-Newtonian Flow in Porous Media

A multigrid adaptive refinement algorithm for non-Newtonian flow in porous media is presented. The saturated flow of a non-Newtonian fluid is described by the continuity equation and the generalized Darcy law. The resulting second order nonlinear elliptic equation is discretized by a finite volume method on a cell-centered grid. A nonlinear full-multigrid, full-approximation-storage algorithm is implemented. As a smoother, a single grid solver based on Picard linearization and Gauss-Seidel relaxation is used. Further, a local refinement multigrid algorithm on a composite grid is developed. A residual based error indicator is used in the adaptive refinement criterion. A special implementation approach is used, which allows us to perform unstructured local refinement in conjunction with the finite volume discretization. Several results from numerical experiments are presented in order to examine the performance of the solver.
Keywords: Nonlinear multigrid, adaptive refinement, non-Newtonian flow in porous media
(17 pages, 2003)

53. S. Kruse

On the Pricing of Forward Starting Options under Stochastic Volatility

We consider the problem of pricing European forward starting options in the presence of stochastic volatility. By performing a change of measure using the asset price at the time of strike determination as a numeraire, we derive a closed-form solution based on Heston's model of stochastic volatility.

Keywords: Option pricing, forward starting options, Heston model, stochastic volatility, cliquet options

(11 pages, 2003)

54. O. Iliev, D. Stoyanov

Multigrid – adaptive local refinement solver for incompressible flows

A non-linear multigrid solver for incompressible Navier-Stokes equations, exploiting finite volume discretization of the equations, is extended by adaptive local refinement. The multigrid is the outer iterative cycle, while the SIMPLE algorithm is used as a smoothing procedure. Error indicators are used to define the refinement subdomain. A special implementation approach is used, which allows to perform unstructured local refinement in conjunction with the finite volume discretization.

The multigrid - adaptive local refinement algorithm is tested on 2D Poisson equation and further is applied to a lid-driven flows in a cavity (2D and 3D case), comparing the results with bench-mark data. The software design principles of the solver are also discussed.

Keywords: Navier-Stokes equations, incompressible flow, projection-type splitting, SIMPLE, multigrid methods, adaptive local refinement, lid-driven flow in a cavity

(37 pages, 2003)

55. V. Starikovicius

The multiphase flow and heat transfer in porous media

In first part of this work, summaries of traditional Multiphase Flow Model and more recent Multiphase Mixture Model are presented. Attention is being paid to attempts include various heterogeneous aspects into models. In second part, MMM based differential model for two-phase immiscible flow in porous media is considered. A numerical scheme based on the sequential solution procedure and control volume based finite difference schemes for the pressure and saturation-conservation equations is developed. A computer simulator is built, which exploits object-oriented programming techniques. Numerical result for several test problems are reported.

Keywords: Two-phase flow in porous media, various formulations, global pressure, multiphase mixture model, numerical simulation

(30 pages, 2003)

56. P. Lang, A. Sarishvili, A. Wirsen

Blocked neural networks for knowledge extraction in the software development process

One of the main goals of an organization developing software is to increase the quality of the software while at the same time to decrease the costs and the duration of the development process. To achieve this, various decisions e.ecting this goal before and during the development process have to be made by the managers. One appropriate tool for decision support are simulation models of the software life cycle, which also help to understand the dynamics of the software development process. Building up a simulation model requires a mathematical description of the interactions between di.erent objects involved in the development process. Based on experimental data, techniques from the .eld of knowledge discovery can be used to quantify these interactions and to generate new process knowledge based on the analysis of the determined relationships. In this paper blocked neuronal networks and related relevance measures will be presented as an appropriate tool for quanti.cation and validation of qualitatively known dependencies in the software development process.

Keywords: Blocked Neural Networks, Nonlinear Regression, Knowledge Extraction, Code Inspection

(21 pages, 2003)

57. H. Knaf, P. Lang, S. Zeiser

Diagnosis aiding in Regulation Thermography using Fuzzy Logic

The objective of the present article is to give an overview of an application of Fuzzy Logic in Regulation Thermography, a method of medical diagnosis support. An introduction to this method of the complementary medical science based on temperature measurements – so-called thermograms – is provided. The process of modelling the physician's thermogram evaluation rules using the calculus of Fuzzy Logic is explained.

Keywords: fuzzy logic,knowledge representation, expert system

(22 pages, 2003)

58. M.T. Melo, S. Nickel, F. Saldanha da Gama

Largescale models for dynamic multi-commodity capacitated facility location

In this paper we focus on the strategic design of supply chain networks. We propose a mathematical modeling framework that captures many practical aspects of network design problems simultaneously but which have not received adequate attention in the literature. The aspects considered include: dynamic planning horizon, generic supply chain network structure, external supply of materials, inventory opportunities for goods, distribution of commodities, facility configuration, availability of capital for investments, and storage limitations. Moreover, network configuration decisions concerning the gradual relocation of facilities over the planning horizon are considered. To cope with fluctuating demands, capacity expansion and reduction scenarios are also analyzed as well as modular capacity shifts. The relation of the proposed modeling framework with existing models is discussed. For problems of reasonable size we report on our computational experience with standard mathematical programming software. In particular, useful insights on the impact of various factors on network design decisions are provided.

Keywords: supply chain management, strategic planning, dynamic location, modeling

(40 pages, 2003)

59. J. Orlik

Homogenization for contact problems with periodically rough surfaces

We consider the contact of two elastic bodies with rough surfaces at the interface. The size of the micropeaks and valleys is very small compared with the macrosize of the bodies' domains. This makes the direct application of the FEM for the calculation of the contact problem prohibitively costly. A method is developed that allows deriving a macrocontact condition on the interface. The method involves the twoscale asymptotic homogenization procedure that takes into account the microgeometry of the interface layer and the stiffnesses of materials of both domains. The macrocontact condition can then be used in a FEM model for the contact problem on the macrolevel. The averaged contact stiffness obtained allows the replacement of the interface layer in the macromodel by the macrocontact condition.

Keywords: asymptotic homogenization, contact problems

(28 pages, 2004)

60. A. Scherrer, K.-H. Küfer, M. Monz, F. Alonso, T. Bortfeld

IMRT planning on adaptive volume structures – a significant advance of computational complexity

In intensity-modulated radiotherapy (IMRT) planning the oncologist faces the challenging task of finding a treatment plan that he considers to be an ideal compromise of the inherently contradictive goals of delivering a sufficiently high dose to the target while widely sparing critical structures. The search for this a priori unknown compromise typically requires the computation of several plans, i.e. the solution of several optimization problems. This accumulates to a high computational expense due to the large scale of these problems - a consequence of the discrete problem formulation. This paper presents the adaptive clustering method as a new algorithmic concept to overcome these difficulties. The computations are performed on an individually adapted structure of voxel clusters rather than on the original voxels leading to a decisively reduced computational complexity as numerical examples on real clinical data demonstrate. In contrast to many other similar concepts, the typical trade-off between a reduction in computational complexity and a loss in exactness can be avoided: the adaptive clustering method produces the optimum of the original problem. This flexible method can be applied to both single- and multi-criteria optimization methods based on most of the convex evaluation functions used in practice.

Keywords: Intensity-modulated radiation therapy (IMRT), inverse treatment planning, adaptive volume structures, hierarchical clustering, local refinement, adaptive clustering, convex programming, mesh generation, multi-grid methods

(24 pages, 2004)

61. D. Kehrwald

Parallel lattice Boltzmann simulation of complex flows

After a short introduction to the basic ideas of lattice Boltzmann methods and a brief description of a modern parallel computer, it is shown how lattice Boltzmann schemes are successfully applied for simulating fluid flow in microstructures and calculating material properties of porous media. It is explained how lattice Boltzmann schemes compute the gradient of the velocity field without numerical differentiation. This feature is then utilised for the simulation of pseudo-plastic fluids, and numerical results are presented for a simple benchmark problem as well as for the simulation of liquid composite moulding.

Keywords: Lattice Boltzmann methods, parallel computing, microstructure simulation, virtual material design, pseudo-plastic fluids, liquid composite moulding

(12 pages, 2004)

62. O. Iliev, J. Linn, M. Moog, D. Niedziela, V. Starikovicius

On the Performance of Certain Iterative Solvers for Coupled Systems Arising in Discretization of Non-Newtonian Flow Equations

Iterative solution of large scale systems arising after discretization and linearization of the unsteady non-Newtonian Navier–Stokes equations is studied. cross WLF model is used to account for the non-Newtonian behavior of the fluid. Finite volume method is used to discretize the governing system of PDEs. Viscosity is treated explicitely (e.g., it is taken from the previous time step), while other terms are treated implicitly. Different preconditioners (block–diagonal, block–triangular, relaxed incomplete LU factorization, etc.) are used in conjunction with advanced iterative methods, namely, BiCGStab, CGS, GMRES. The action of the preconditioner in fact requires inverting different blocks. For this purpose, in addition to preconditioned BiCGStab, CGS, GMRES, we use also algebraic multigrid method (AMG). The performance of the iterative solvers is studied with respect to the number of unknowns, characteristic velocity in the basic flow, time step, deviation from Newtonian behavior, etc. Results from numerical experiments are presented and discussed.

Keywords: Performance of iterative solvers, Preconditioners, Non-Newtonian flow

(17 pages, 2004)

63. R. Ciegis, O. Iliev, S. Rief, K. Steiner

On Modelling and Simulation of Different Regimes for Liquid Polymer Moulding

In this paper we consider numerical algorithms for solving a system of nonlinear PDEs arising in modeling of liquid polymer injection. We investigate the particular case when a porous preform is located within the mould, so that the liquid polymer flows through a porous medium during the filling stage. The nonlinearity of the governing system of PDEs is due to the non-Newtonian behavior of the polymer, as well as due to the moving free boundary. The latter is related to the penetration front and a Stefan type problem is formulated to account for it. A finite-volume method is used

to approximate the given differential problem. Results of numerical experiments are presented.
We also solve an inverse problem and present algorithms for the determination of the absolute preform permeability coefficient in the case when the velocity of the penetration front is known from measurements. In both cases (direct and inverse problems) we emphasize on the specifics related to the non-Newtonian behavior of the polymer. For completeness, we discuss also the Newtonian case. Results of some experimental measurements are presented and discussed.
Keywords: Liquid Polymer Moulding, Modelling, Simulation, Infiltration, Front Propagation, non-Newtonian flow in porous media
(43 pages, 2004)

64. T. Hanne, H. Neu

Simulating Human Resources in Software Development Processes

In this paper, we discuss approaches related to the explicit modeling of human beings in software development processes. While in most older simulation models of software development processes, esp. those of the system dynamics type, humans are only represented as a labor pool, more recent models of the discrete-event simulation type require representations of individual humans. In that case, particularities regarding the person become more relevant. These individual effects are either considered as stochastic variations of productivity, or an explanation is sought based on individual characteristics, such as skills for instance. In this paper, we explore such possibilities by recurring to some basic results in psychology, sociology, and labor science. Various specific models for representing human effects in software process simulation are discussed.
Keywords: Human resource modeling, software process, productivity, human factors, learning curve
(14 pages, 2004)

65. O. Iliev, A. Mikelic, P. Popov

Fluid structure interaction problems in deformable porous media: Toward permeability of deformable porous media

In this work the problem of fluid flow in deformable porous media is studied. First, the stationary fluid-structure interaction (FSI) problem is formulated in terms of incompressible Newtonian fluid and a linearized elastic solid. The flow is assumed to be characterized by very low Reynolds number and is described by the Stokes equations. The strains in the solid are small allowing for the solid to be described by the Lame equations, but no restrictions are applied on the magnitude of the displacements leading to strongly coupled, nonlinear fluid-structure problem. The FSI problem is then solved numerically by an iterative procedure which solves sequentially fluid and solid subproblems. Each of the two subproblems is discretized by finite elements and the fluid-structure coupling is reduced to an interface boundary condition. Several numerical examples are presented and the results from the numerical computations are used to perform permeability computations for different geometries.
Keywords: fluid-structure interaction, deformable porous media, upscaling, linear elasticity, stokes, finite elements
(23 pages, 2004)

66. F. Gaspar, O. Iliev, F. Lisbona, A. Naumovich, P. Vabishchevich

On numerical solution of 1-D poroelasticity equations in a multilayered domain

Finite volume discretization of Biot system of poroelasticity in a multilayered domain is presented. Staggered grid is used in order to avoid nonphysical oscillations of the numerical solution, appearing when a collocated grid is used. Various numerical experiments are presented in order to illustrate the accuracy of the finite difference scheme. In the first group of experiments, problems having analytical solutions are solved, and the order of convergence for the velocity, the pressure, the displacements, and the stresses is analyzed. In the second group of experiments numerical solution of real problems is presented.
Keywords: poroelasticity, multilayered material, finite volume discretization, MAC type grid
(41 pages, 2004)

67. J. Ohser, K. Schladitz, K. Koch, M. Nöthe

Diffraction by image processing and its application in materials science

A spectral theory for constituents of macroscopically homogeneous random microstructures modeled as homogeneous random closed sets is developed and provided with a sound mathematical basis, where the spectrum obtained by Fourier methods corresponds to the angular intensity distribution of x-rays scattered by this constituent. It is shown that the fast Fourier transform applied to three-dimensional images of microstructures obtained by micro-tomography is a powerful tool of image processing. The applicability of this technique is is demonstrated in the analysis of images of porous media.
Keywords: porous microstructure, image analysis, random set, fast Fourier transform, power spectrum, Bartlett spectrum
(13 pages, 2004)

68. H. Neunzert

Mathematics as a Technology: Challenges for the next 10 Years

No doubt: Mathematics has become a technology in its own right, maybe even a key technology. Technology may be defined as the application of science to the problems of commerce and industry. And science? Science maybe defined as developing, testing and improving models for the prediction of system behavior; the language used to describe these models is mathematics and mathematics provides methods to evaluate these models. Here we are! Why has mathematics become a technology only recently? Since it got a tool, a tool to evaluate complex, "near to reality" models: Computer! The model may be quite old – Navier-Stokes equations describe flow behavior rather well, but to solve these equations for realistic geometry and higher Reynolds numbers with sufficient precision is even for powerful parallel computing a real challenge. Make the models as simple as possible, as complex as necessary – and then evaluate them with the help of efficient and reliable algorithms: These are genuine mathematical tasks.
Keywords: applied mathematics, technology, modelling, simulation, visualization, optimization, glass processing, spinning processes, fiber-fluid interaction, trubulence effects, topological optimization, multicriteria optimization, Uncertainty and Risk, financial mathematics, Malliavin calculus, Monte-Carlo methods, virtual material design, filtration, bio-informatics, system biology
(29 pages, 2004)

69. R. Ewing, O. Iliev, R. Lazarov, A. Naumovich

On convergence of certain finite difference discretizations for 1D poroelasticity interface problems

Finite difference discretizations of 1D poroelasticity equations with discontinuous coefficients are analyzed. A recently suggested FD discretization of poroelasticity equations with constant coefficients on staggered grid, [5], is used as a basis. A careful treatment of the interfaces leads to harmonic averaging of the discontinuous coefficients. Here, convergence for the pressure and for the displacement is proven in certain norms for the scheme with harmonic averaging (HA). Order of convergence 1.5 is proven for arbitrary located interface, and second order convergence is proven for the case when the interface coincides with a grid node. Furthermore, following the ideas from [3], modified HA discretization are suggested for particular cases. The velocity and the stress are approximated with second order on the interface in this case. It is shown that for wide class of problems, the modified discretization provides better accuracy. Second order convergence for modified scheme is proven for the case when the interface coincides with a displacement grid node. Numerical experiments are presented in order to illustrate our considerations.
Keywords: poroelasticity, multilayered material, finite volume discretizations, MAC type grid, error estimates
(26 pages,2004)

70. W. Dörfler, O. Iliev, D. Stoyanov, D. Vassileva

On Efficient Simulation of Non-Newtonian Flow in Saturated Porous Media with a Multigrid Adaptive Refinement Solver

Flow of non-Newtonian in saturated porous media can be described by the continuity equation and the generalized Darcy law. Efficient solution of the resulting second order nonlinear elliptic equation is discussed here. The equation is discretized by a finite volume method on a cell-centered grid. Local adaptive refinement of the grid is introduced in order to reduce the number of unknowns. A special implementation approach is used, which allows us to perform unstructured local refinement in conjunction with the finite volume discretization. Two residual based error indicators are exploited in the adaptive refinement criterion. Second order accurate discretization on the interfaces between refined and non-refined subdomains, as well as on the boundaries with Dirichlet boundary condition, are presented here, as an essential part of the accurate and efficient algorithm. A nonlinear full approximation storage multigrid algorithm is developed especially for the above described composite (coarse plus locally refined) grid approach. In particular, second order approximation around interfaces is a result of a quadratic approximation of slave nodes in the multigrid - adaptive refinement (MG-AR) algorithm. Results from numerical solution of various academic and practice-induced problems are presented and the performance of the solver is discussed.
Keywords: Nonlinear multigrid, adaptive renement, non-Newtonian in porous media
(25 pages, 2004)

71. J. Kalcsics, S. Nickel, M. Schröder

Towards a Unified Territory Design Approach – Applications, Algorithms and GIS Integration

Territory design may be viewed as the problem of grouping small geographic areas into larger geographic clusters called territories in such a way that the latter are acceptable according to relevant planning criteria. In this paper we review the existing literature for applications of territory design problems and solution approaches for solving these types of problems. After identifying features common to all applications we introduce a basic territory design model and present in detail two approaches for solving this model: a classical location–allocation approach combined with optimal split resolution techniques and a newly developed computational geometry based method. We present computational results indicating the efficiency and suitability of the latter method for solving large–scale practical problems in an interactive environment. Furthermore, we discuss extensions to the basic model and its integration into Geographic Information Systems.
Keywords: territory desgin, political districting, sales territory alignment, optimization algorithms, Geographical Information Systems
(40 pages, 2005)

72. K. Schladitz, S. Peters, D. Reinel-Bitzer, A. Wiegmann, J. Ohser

Design of acoustic trim based on geometric modeling and flow simulation for non-woven

In order to optimize the acoustic properties of a stacked fiber non-woven, the microstructure of the non-woven is modeled by a macroscopically homogeneous random system of straight cylinders (tubes). That is, the fibers are modeled by a spatially stationary random system of lines (Poisson line process), dilated by a sphere. Pressing the non-woven causes anisotropy. In our model, this anisotropy is described by a one parametric distribution of the direction of the fibers. In the present application, the anisotropy parameter has to be estimated from 2d reflected light microscopic images of microsections of the non-woven.
After fitting the model, the flow is computed in digitized realizations of the stochastic geometric model using the lattice Boltzmann method. Based on the flow resistivity, the formulas of Delany and Bazley predict the frequency-dependent acoustic absorption of the non-woven in the impedance tube.

Using the geometric model, the description of a non-woven with improved acoustic absorption properties is obtained in the following way: First, the fiber thicknesses, porosity and anisotropy of the fiber system are modified. Then the flow and acoustics simulations are performed in the new sample. These two steps are repeatedc for various sets of parameters. Finally, the set of parameters for the geometric model leading to the best acoustic absorption is chosen.
Keywords: random system of fibers, Poisson line process, flow resistivity, acoustic absorption, Lattice-Boltzmann method, non-woven
(21 pages, 2005)

Status quo: February 2005